https://doi.org/10.5194/essd-2025-812
Preprint. Discussion started: 15 January 2026

Open Access Earth System Science Data Discussions

The WoKaS-Iso Database: Workflow for a Global Compilation of Oxygen-18 and Deuterium Records in Karst Springs and Cave Drip Water for Enhanced Understanding of Karst Systems

Yining Zang[1]*, Pauline C.Treble[2,3]*, Kei Yoshimura[4,5], Jayson Gabriel Pinza[6,7], Fengbo Zhang[8], Kübra Özdemir Çallı[1], Xiaojun Mei[9], Admin Husic[10], Alena Gessert[11], Andrej Stroj[12], Bartolomé Andreo[13], Bernard Ladouche[14,15,], Christine Stumpp[16], Diana Mance[17], Eleni Zagana[18], Fen Huang[19], Giuseppe Sappa[20], Harald Kunstmann[21,22], Heike Brielmann[23], Hong Zhou[24], Huaying Wu[19], Jakob Garvelmann[21,25], James Berglund[26], Jean-Baptiste Charlier[14,15], Jens Lange[27], Juan Antonio Barberá Fornell[13], Junbing Pu[28], Konstantina Katsanou[29], Kun Ren[19], Laura Toran[30], Laurence Gill[31], Maria Filippini[32], Martin Kralik[33], Matías Mudarra Martínez[13], Min Zhao[34], Mingming Luo[24], Nico Goldscheider[35], Nikolaos Lambrakis[18], Pantaleone De Vita[36], Qiong Xiao[19], Shi Yu[19], Silvia Iacurto[20], Silvio Coda[36], Ted McCormack[37], Vincenzo Allocca[36], W. George Darling[38], Walter D'Alessandro[39], Xulei Guo[24], Yundi Hu[40], Zhijun Wang[41], Eva Kaminsky[42,43], Jiří Faimon[44,45], Marek Lang[44], Pavel Pracný[44], Andreas Hartmann[1]

* Corresponding authors

[1]Institute of Groundwater Management, Technical University of Dresden, Dresden, 01069, Germany
[2]ANSTO, New Illawarra Road, Lucas Heights, NSW 2234, Australia
[3]School of Biological, Earth and Environmental Sciences, UNSW Sydney, Sydney NSW, 2052, Australia
[4]Institute of Industrial Science, The University of Tokyo, Kashiwa, Japan
[5]Japan Atmosphere and Ocean Research Institute, The University of Tokyo, Kashiwa, Japan
[6]ECOSPHERE Research Group, University of Antwerp, Universiteitsplein 1C, 2610 Antwerp, Belgium
[7]Division of Soil and Water Management, KU Leuven, Celestijnenlaan 200E, 3001 Leuven, Belgium
[8]Ningbo River Management Center, Ningbo Water Resources Bureau, Ningbo 315000, China
[9]Merchant Marine College, Shanghai Maritime University, Shanghai 201306, China
[10]Department of Civil and Environmental Engineering, Virginia Tech, Blacksburg 24061, USA
[11]Institute of Geography, Faculty of Sciences, University of P.J. Šafárik, 040 01 Košice, Slovakia
[12]Croatian Geological Survey, Sachsova 2, 10000 Zagreb, Croatia
[13]Department of Geology and Centre of Hydrogeology at the University of Malaga, 29071, Malaga, Spain
[14]BRGM, Univ Montpellier, Montpellier, France
[15]G-EAU, Univ Montpellier, AgroParisTech, BRGM, CIRAD, INRAE, Institut Agro, IRD, Montpellier, France
[16]Institute of Soil Physics and Rural Water Management, Department of Landscape, Water and Infrastructure, BOKU University, Vienna, Austria
[17]Faculty of Physics, University of Rijeka, 51000, Rijeka, Croatia
[18]Laboratory of Hydrogeology, Department of Geology, Faculty of Natural Sciences, University of Patras, GR-26504 Patras, Greece
[19]Key Laboratory of Karst Dynamics, MNR and GZAR, Institute of Karst Geology, Chinese Academy of Geological Sciences, Guilin, 541004, China
[20]Department of Civil, Constructional and Environmental Engineering (DICEA), Sapienza University of Rome, 00184 Rome, Italy
[21]Institute of Meteorology and Climate Research, Karlsruhe Institute of Technology, Campus Alpin, D-82467 Garmisch-Partenkirchen, Germany
[22]Institute of Geography, University of Augsburg, D-86135 Augsburg, Germany
[23]Environment Agency Austria, Groundwater Unit, Spittelauer Laende 5, A-1090 Vienna, Austria

https://doi.org/10.5194/essd-2025-812
Preprint. Discussion started: 15 January 2026

[24]School of Environmental Studies& Institute of Geological Survey, China University of Geosciences, Wuhan, 430074, Hubei, China
[25]Boden & grundwasser Allgäu GmbH, D-87527 Sonthofen, Germany
[26]Department of Civil and Environmental Engineering, University of Wisconsin – Platteville, Platteville, Wisconsin, USA
[27]Hydrology, University of Freiburg, 79098 Freiburg, Germany
[28]Chongqing Key Laboratory of Carbon Cycle and Carbon Regulation of Mountain Ecosystem, School of Geography and Tourism, Chongqing Normal University, Chongqing, 401331, China
[29]Department of Water Resources and Ecosystems, IHE Delft Institute for Water Education, Delft, Netherlands
[30]Department of Earth and Environmental Science, Temple University, Philadelphia, Pennsylvania, USA
[31]Department of Civil, Structural and Environmental Engineering, Trinity College Dublin, Ireland
[32]Department of Biological, Geological and Environmental Sciences—BiGeA, Alma Mater Studiorum, University of Bologna, Via Selmi 3, 40126 Bologna, Italy
[33]Department of Environmental Geosciences, Center for Microbiology and Environmental Systems Science, University of Vienna, 1090 Vienna, Austria
[34]State Key Laboratory of Environmental Geochemistry (SKLEG), Institute of Geochemistry, Chinese Academy of Sciences (CAS), Guiyang, China
[35]Institute of Applied Geosciences, Karlsruhe Institute of Technology, D-76131 Karlsruhe, Germany
[36]Department of Earth, Environmental and Resources Sciences (DiSTAR), University of Naples Federico II, Naples, Italy
[37]Geological Survey Ireland, Booterstown Avenue, Booterstown, Blackrock, Ireland
[38]British Geological Survey, Wallingford OX10 8BB, United Kingdom
[39]Istituto Nazionale di Geofisica e Vulcanologia – Sezione di Palermo, Via La Malfa 153, 90146 Palermo, Italy
[40]School of Geography and Environmental Science, Guizhou Normal University, Guiyang 550001, People's Republic of China
[41]Faculty of Arts and Sciences, Beijing Normal University, Zhuhai 519087, China
[42]Karst and Cave Group, Geological Paleontological Department, Natural History Museum, Vienna, Austria
[43]Institute of Soil Physics and Rural Water Management, Department of Landscape, Water and Infrastructure, BOKU University, Vienna, Austria
[44]Department of Geological Sciences, Faculty of Science, Masaryk University, Brno, Czech Republic
[45]Czech Geological Survey, Brno Branch, Brno, Czech Republic

Correspondence to: Yining Zang (yining.zang@tu-dresden.de), Pauline C.Treble (ptr@ansto.gov.au)

Abstract

For analysing karst hydrogeological systems, observations of karst springs and cave drips are considered indispensable. In addition to hydrometric observations, knowing the oxygen and hydrogen stable isotope ratios has improved the understanding of vadose zone and aquifer dynamics, likewise supporting system characterisation and modelling. However, limited accessibility and high costs of the analysis of stable isotopes in karst aquifers have hindered progress in karst research and impeded the accurate understanding of karst processes especially when it comes to comparative or large-scale studies. In this study, we present our workflow to compile the WoKaS-Iso database, the first extensive collection of time series data for Oxygen-18 and Deuterium isotopes in karst springs and cave drip water from diverse sources, encompassing publications, theses, reports, online archives, and collaborative initiatives worldwide. The database incorporates data sourced from 236 springs and 74 caves, comprising in total 997 time series (379 time series for the springs and 618 time series for the cave drip water). These datasets provide coverage across significant karst regions globally, spanning China, the USA, Europe, the Middle East, and Australia. Within datasets, 79% for springs and 68% for cave drip water exhibit resolutions finer than monthly

intervals. In addition, by integrating isotopic records with ancillary environmental variables including spring discharge, cave drip rate, precipitation, and rainwater isotopes, the database offers a more comprehensive perspective on hydrological behaviours in karst aquifers, hence advancing hydrogeological characterisation and modelling. The WoKaS-Iso database not only deepens the understanding of the complex systems but also promotes sustainable water resource management as well as the potential to foster collaborative research. The database can be accessed at: https://doi.org/10.25532/OPARA-909 (Zang, 2025).

1 Introduction

Carbonate rock areas, particularly those with highly karstified systems, serve as a critical source of potable water, catering 10%–25% of the global population (Ford and Williams, 2007; Stevanović, 2019) and up to 50% in some countries (European Cooperation in Science and Technology, 1995). Beyond water supply, these aquifers encompass extensive cave networks that preserve valuable paleoclimate records, reflecting key variability patterns of past environmental conditions (McDermott, 2004). The karstification leads to inherent structural heterogeneity and strong nonlinearities of hydraulic properties (Frank et al., 2021; Jourde et al., 2018; Labat et al., 2016) that drive subsurface water flow regimes and storage mechanisms including fast conduit turbulent flow and slow matrix storage (Bakalowicz, 2005; Goldscheider and Drew, 2007) while challenging characterization of karst aquifer structures, hydraulic dynamics, and contamination pathways. Consequently, a comprehensive understanding of hydrogeological behaviours in karst systems is essential for sustainable water resource management and protection. This is also a matter of urgency for certain European regions that appear to be sensitive to the effects of global warming(Giese et al., 2025).

Stable isotopes of oxygen and hydrogen, being part of the water molecule itself, are ideal tracers for identifying water sources (Hartmann et al., 2014) delineating subsurface flow paths, estimating transit times (Liu and Yamanaka, 2012; McDonnell et al., 2010), and quantifying mixing processes (Rusjan et al., 2019). In karst hydrogeology, spring isotope signatures integrating responses from both saturated and unsaturated zones often give additional information about complex recharge patterns that are not captured by discharge data alone. Isotope data thus provide critical complementary information to resolve flow and transport dynamics. Meanwhile, in speleological research, stable isotopes are central to understanding recharge processes through the epikarst, providing a distinctive window into unsaturated zone and recharge processes (Hartmann and Baker, 2017). Cave drips act as a medium to monitor flow path through epikarst that is directly linked to climate signals preserved in speleothem formed from cave drips which can serve as archives for paleoclimate reconstruction (Bradley et al., 2010; (MacDermott et al., 2006). Long-term rainfall and drip water monitoring is crucial for distinguishing local or regional climatic influences on cave system isotope variability (Pape et al., 2010). Moreover, stable isotopes provide critical information on water transit times through karst systems, allowing the identification of fast conduit flow versus slow matrix storage contributions. This capability is essential for understanding the temporal dynamics of recharge, flow pathways, and aquifer vulnerability to contamination, as it directly links precipitation events to spring or cave drip responses. Incorporating isotope-based transit time estimates into hydrological models enhances the characterization of flow heterogeneity and improves predictions of contaminant transport and residence times within karst aquifers.

More recently, isotope-based models have emerged to couple hydrological dynamics with stable isotopes (Birkel and Soulsby, 2015; Zhang et al., 2019). Andreo et al. (2004) applied $\delta^{18}O$ and $\delta^{2}H$ in precipitation and groundwater to determine the water origin and understand the aquifer dynamics in the Yunquera-Nieves karstic massif in Spain. Wang et al. (2022) coupled hydrochemical and stable isotopic compositions to identify the groundwater hydrochemistry evolution in the Western Yellow Sea Coast of China. Hartmann et al. (2012) utilized isotopic information ($\delta^{18}O$) to calibrate their recharge model. Hydrological functions such as water storage, flux and water age distributions are effectively quantified by these isotope-coupled models, providing essential indicators of understanding the behaviour of the karst aquifer (Mayer-Anhalt et al., 2022). Additionally, coupling isotopic and hydrological data has proven valuable for facilitating the multi-objective calibration and validation (Hartmann et al., 2013) enhancing the model evaluation, mitigating overparameterization and reducing the potential uncertainties (Li et al., 2022; Zhang et al., 2019). On the other hand, recent cave-based research has used stable water isotopes to advance the understanding of karst vadose zone hydrology. Priestley et al. (2023) combined $\delta^{18}O$ from speleothems and drip waters with modelled soil moisture data to show how regional drying in southwestern Australia disrupted rainfall recharge to shallow karst aquifers—an unprecedented shift over the past 800 years. Baker et al. (2019) analyzed $\delta^{18}O$ from 163 global drip sites and found that in seasonal climates, drip water isotopes reflect recharge-weighted precipitation, refining the interpretation of speleothem records. Treble et al. (2022) demonstrated that isotopic variability within caves is largely driven by differences in flow path properties—fracture versus matrix flow—highlighting the importance of hydrological heterogeneity in shaping $\delta^{18}O$ signals. Together, these studies underline the growing potential of isotope-hydrology approaches for resolving spatial and temporal variability in karst recharge and for reconstructing past hydroclimatic conditions. All these applications highlight the growing value of isotopic datasets for both process understanding and model development in karst systems.

Several global databases have been established to archive stable water isotope data, most notably the Global Network of Isotopes in Precipitation (GNIP) and the Global Network of Isotopes in Rivers (GNIR) maintained by the International Atomic Energy Agency (IAEA) and World Meteorological Organization (WMO). In addition, Staudinger et al. (2020) developed a long-term $\delta^{18}O$ and $\delta^{2}H$ database for streamflow and precipitation for 23 catchments in Switzerland, and Li et al. (2025) established the first global surface water stable isotope database from measured data, web-sourced records and referenced data. While these databases provide essential insights into hydrological processes, they largely omit $\delta^{18}O$ and $\delta^{2}H$ data from karst springs and cave drip waters. $\delta^{18}O$ and $\delta^{2}H$ signatures in karst springs and cave drip waters as natural tracers have been proven invaluable, offering insights into characterizing recharge patterns, validating and enhancing the accuracy of hydrological models and calibrating the reconstruction of paleoclimate through speleothem records (Tremaine et al., 2011). Despite the

https://doi.org/10.5194/essd-2025-812
Preprint. Discussion started: 15 January 2026

significance, the broader use of isotopic applications remained constrained by the high cost of stable isotope analysis and limited accessibility to the existing datasets for large-scale modelling and comparative studies across karst regions.

To allow more a broader application and comparative studies, we developed the WoKaS-Iso - a global compilation of the time series of stable isotope ($\delta^{18}O$ and δ^2H) records from karst springs and cave drip water. As complementary information, this database also includes the karst discharge, drip rate, precipitation, and precipitation $\delta^{18}O$ and δ^2H observations. For springs, datasets were aggregated from collaborators, reviewed publications, technical reports and theses. For caves, data were sourced from the SISAL_mon_v1 cave drip monitoring database (Treble et al., to be submitted), under consistent formatting and quality control. Metadata considered karst springs and cave name, geological information of sites, monitoring starting and ending date, observation length and data source details. We present the methodology of WoKaS-Iso database construction, describe datasets records, datasets quality control, data usage notes, and discuss its applications and outlook. Furthermore, we evaluate the performance of three global precipitation isotope models, offering the perspectives of model selection in karst hydrology.

2 Data records and methodology

The WoKaS-Iso database is built upon the foundational WoKaS (World Karst Spring hydrograph) database, the first global repository of karst discharge records encompassing over 400 karst springs (Olarinoye et al., 2020). WoKaS-Iso extends this framework by comprising stable isotope data ($\delta^{18}O$ and δ^2H) for karst springs, initially developed from a compilation of 119 stable isotope time series from Europe (Hartmann et al., 2021), the database now aims to expand this initiative to a global scale. For extending the spring isotopes dataset with cave drip water isotopes and drip rate observations, and corresponding rainfall observations, we collaborated with the SISAL (Speleothem Isotope Synthesis and Analysis) working group (https://pastglobalchanges.org/science/wg/sisal/intro). Data acquisition relied primarily on the SISAL_mon_v1 cave drip water database (Treble et al., to be submitted), supplemented by additional processing efforts within the WoKaS-Iso framework to standardize and structure all drip-water time series and rainfall datasets for full interoperability and cross-referencing with the broader WoKaS-Iso framework. In total, 66 cave sites originating from SISAL_mon_v1, together with newly integrated cave monitoring sites from other published and contributed sources were standardized following the WoKaS-Iso data scheme. WoKaS-Iso also synthesizes paired hydrological and climatic parameters datasets including karst spring discharge, rainfall, and rainwater isotopes to support interpretation of the water isotope signature. These datasets were gathered from peer-reviewed publications, theses, reports and research collaborators. In addition to site-based observations, we integrated modelled climatic datasets from gridded global products, including precipitation amount (MSWEP), air temperature (ERA5), evapotranspiration (GLEAM), and precipitation isotopes models (IsoGSM, Isoscape, Sine Curve). Where observed data were unavailable, the precipitation amount and precipitation isotopes from nearby GNIP stations were used as substitutes.

https://doi.org/10.5194/essd-2025-812
Preprint. Discussion started: 15 January 2026

Open Access Earth System Science Data Discussions

From a modelling perspective, the datasets in WoKaS-Iso are organized in two main categories: **system output data** (spring isotopes, spring discharge, cave drip isotopes, cave drip rate) and **system input data** (precipitation amounts, precipitation isotopes). The overview workflow of WoKaS-Iso database creation is illustrated in Fig.1.

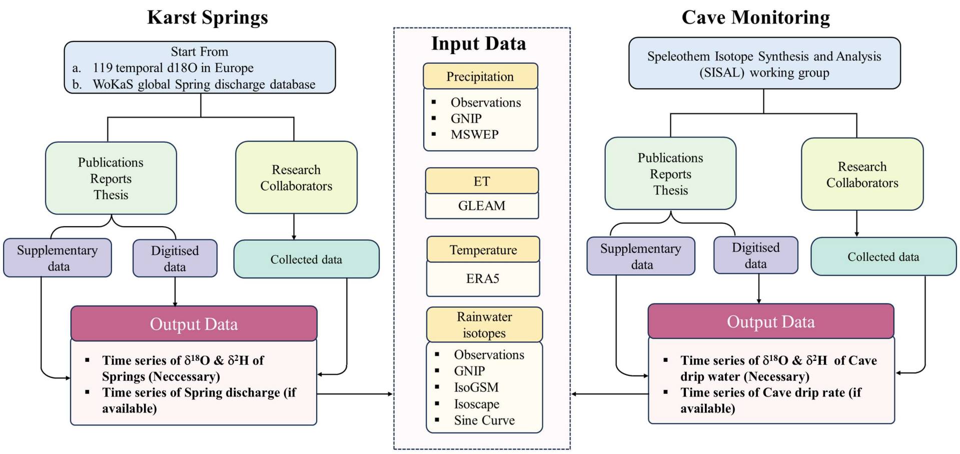

Figure 1: Workflow of the karst spring and cave drip water stable isotopes database construction

2.1 System output data

2.1.1 Available data types

The WoKaS-Iso database compiles observations of oxygen ($\delta^{18}O$) and hydrogen ($\delta^{2}H$), expressed in delta (δ) notation relative to the Vienna Standard Mean Ocean Water (VSMOW), from 236 karst springs and 74 caves accommodating in total 365 drip observation points (e.g., different speleothems). In addition, WoKaS-Iso includes associated karst spring discharge, cave drip rate, precipitation amounts observations and precipitation isotope observations for karst springs and cave sites. Table 1 details the number of time series included in the database for various variables.

https://doi.org/10.5194/essd-2025-812
Preprint. Discussion started: 15 January 2026

Table 1: Summary of WoKaS-Iso database observations

Variables	Karst Springs	Cave Drips	Total
$\delta^{18}O$ Time Series	232	339	571
$\delta^{2}H$ Time Series	147	279	426
Flow Rate Time Series	122	186	308
Precipitation Amounts	119	58	177
Precipitation Isotopes	122	66	188

Among 236 karst springs, 122 (52%) are accompanied by discharge data. Of these, 95 springs include both discharge and output $\delta^{18}O$ and $\delta^{2}H$ data, while 27 springs possess discharge data paired with either $\delta^{18}O$ or $\delta^{2}H$ measurements. The remaining 114 springs (48%) include only output isotope data: 48 springs with both $\delta^{18}O$ and $\delta^{2}H$ data, and 66 with either $\delta^{18}O$ or $\delta^{2}H$ data. Within 74 caves, one cave includes input data alone but lacks output data. 73 caves comprise 365 drip sites, among these, 161 drip sites (44%) combine drip rate with drip water isotope data, of 161 drip sites, 154 drip sites have drip rate along with $\delta^{18}O$ and $\delta^{2}H$ measurements, while 7 drip sites have drip rate and only $\delta^{18}O$ data. Additionally, 25 drip sites (7%) were measured containing drip rate only. Furthermore, 178 drip sites (49%) contain drip water isotope data alone, 125 drip sites with both $\delta^{18}O$ and $\delta^{2}H$ data, 53 drip sites with $\delta^{18}O$ only. In addition, the database includes 122 time series of rainwater isotopes, and 119 time series of rainfall associated with karst springs, as well as 66 time series of rainwater isotopes and 58 time series of rainfall associated with cave sites. The complete list of karst springs and caves included in the database, along with their coordinates and referenced literatures, are presented in Table S1 and Table S2 in the supplement.

2.1.2 Origin of the collected data

Fig.2 illustrates the sources of the karst spring and cave drip data, respectively. For the karst springs, 90% isotopes data are raw observations while 10% are digitized (extracted from a reference paper). The corresponding karst spring discharge data consists of 86% raw data from collaborators, WoKaS discharge database or online open-access national database. For the rainwater isotopes, 8% of the data are from local measurements, 44% from weather stations, and 48% from global isotope model products. Besides, 50% rainfall data are sourced from local and meteorological data. In terms of cave drip waters, 96% of drip water isotopes derive from direct field measurements, with only 4% digitized. A parallel distribution is observed for drip rate records, where 72% source from observations. In case of rainwater, the majority of rainwater isotopes are obtained from both local sampling campaigns and meteorological stations, with approximately 45% originating from local observations. Likewise, 78% of rainfall data are acquired from local records and meteorological station datasets.

https://doi.org/10.5194/essd-2025-812
Preprint. Discussion started: 15 January 2026

Open Access Earth System Science Data Discussions

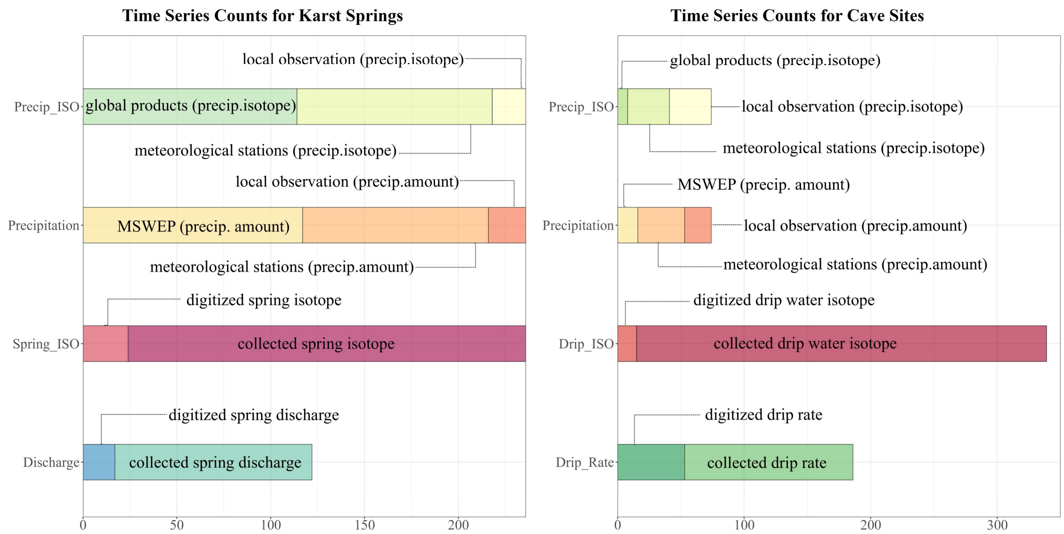

Figure 2: Distribution of time series counts for hydrological and isotopic datasets in WoKaS-Iso database, categorized by source types. For karst springs, precipitation isotopes come from local observations (18), meteorological stations (104), and global model products (114), while precipitation amounts come from local observations (20), meteorological stations (99), and MSWEP (117). Spring water isotopes include collected (212) and digitized (24) data, and spring discharge includes collected (105) and digitized (17) data. For caves, precipitation isotopes come from local observations (33), meteorological stations (33), and global model products (8). Cave drip water isotopes include collected (324) and digitized (15) data, and cave drip rates include collected (133) and digitized (53) data.

Karst Springs: the time series of $\delta^{18}O$ and $\delta^{2}H$ output data were collected from (1) published data in peer-reviewed literatures, scientific reports and academic theses; (2) research collaborators from the network. **Published data**: The publications containing stable isotopes time series data for karst springs were identified through systematic searches of academic databases and web search engines using targeted keywords (e.g. "karst spring isotopes"). Some isotope datasets were obtained directly from the supplementary documents accompanying these publications. For the data not readily accessible, requests were sent to the corresponding authors to solicit contributions to the database. In cases where no response was received, the datasets were digitized from figures in scientific articles, reports and theses using WebplotDigitizer (Rohatgi, 2025), a web-based open-source tool for data extraction. To maximum digitization accuracy, high-quality figures in articles were retrieved programmatically. The extracted datasets were then visually validated by replotting and comparing them with the original figures to ensure the trends' consistency. **Research collaborators**: To further enrich the WoKaS-Iso database, additional data were acquired through communications with research project partners and institutional collaborations. Advertisements were disseminated to relevant academic departments, organizations and researchers. Furthermore, calls for contribution were made to the karst community through poster and oral presentations during the international conferences and workshops. In addition to the sources above, the corresponding karst discharge data were obtained from the online national database such as the U.S. Geological Survey (USGS)'s National Water Information System, and Austria's Bundesministerium für Nachhaltigkeit und Tourismus (eHYD) database.

Cave Monitoring: The compilation of cave drip water isotopes and drip rate for the WoKaS-Iso database followed a structured workflow analogous to that of karst springs. In collaboration with SISAL (Kaushal et al., 2024), data acquisition primarily drew upon the SISAL_mon_v1 (Treble et al., to be submitted), which provided a key foundation for this component. GNIP station data excluded from SISAL_mon_v1 (as noted in the SISAL workbooks) are retained in WoKaS_Iso to preserve the completeness and representativeness of the original monitoring datasets. For some caves, SISAL_mon_v1 includes only the drip water isotope data provided by the authors, but the original drip rate measurements were not available. To address this, WoKaS-Iso digitized the drip rate information from figures in the publications and incorporated these data into the database, thereby enabling quantitative analyses of cave hydrology, drip water dynamics, and speleothem formation processes. Furthermore, additional cave monitoring sites, independent of SISAL_mon_v1, have been incorporated from published studies and research collaborators. All cave drip water datasets were systematically standardised and additional quality control according to the WoKaS-Iso protocol (see chapter 4) was applied. For datasets originating from SISAL_mon_v1, this quality control focused on additional harmonisation and alignment with the WoKaS-Iso structure, building on the quality control already performed in Treble et al. (to be submitted). The datasets were then organised within a structure specifically designed to ensure interoperability with the broader WoKaS-Iso. To ensure transparency and facilitate cross-referencing, the corresponding SISAL_mon_v1 cave identifiers are provided in the WoKaS-Iso metadata tables where applicable. Additional information on the cave drip water data collection methodology and site selection in SISAL_mon_v1 is provided in Treble et al. (to be submitted).

2.1.3 Description of available datasets

The spatial distributions of springs and caves within the database are shown in Fig.3 together with the World Karst Aquifer Map (WOKAM) (Chen et al., 2017). The locations in the database are primarily situated across key global karst regions including China, Europe, Australia, the Middle East and the USA. We summarised the detailed statistics of data type combinations of 236 springs and 339 cave drip sites with isotopic data records in Fig.4, stratified by the predominant karst areas identified in Fig.3. Springs are analysed for China, the USA, Europe for springs, while cave drip sites are grouped by China, Australia, and Europe. The stacked histograms display the distribution of dataset types across these regions and align with the regional distribution trend described in the preceding section.

Most of karst spring records are collected in Europe with approximately 50% of them accompanied by discharge measurements (Fig. 4a). Fewer springs, but a similar composition of the records is observed in China, where roughly half of the spring locations include discharge data. Whereas only about one-third of springs in the USA have associated discharge data. For karst

https://doi.org/10.5194/essd-2025-812
Preprint. Discussion started: 15 January 2026

Open Access Earth System Science Data Discussions

springs in other regions, the proportion with discharge data is higher, up to 83%. As for isotopic time series, portions of spring datasets containing both $\delta^{18}O$ and $\delta^{2}H$ is 86% in China, 70% in the USA and 62% in other countries. Fig. 4b shows that the majority of cave drip sites in China include drip rate observations. Almost half of the drip sites in Australia and Europe incorporate drip rate data, while the proportion is lower in other regions (only around 30%). Furthermore, more than 95% cave drips were measured for both $\delta^{18}O$ and $\delta^{2}H$ data in China and Australia; the proportion exceeds 70% in Europe and other regions.

https://doi.org/10.5194/essd-2025-812
Preprint. Discussion started: 15 January 2026

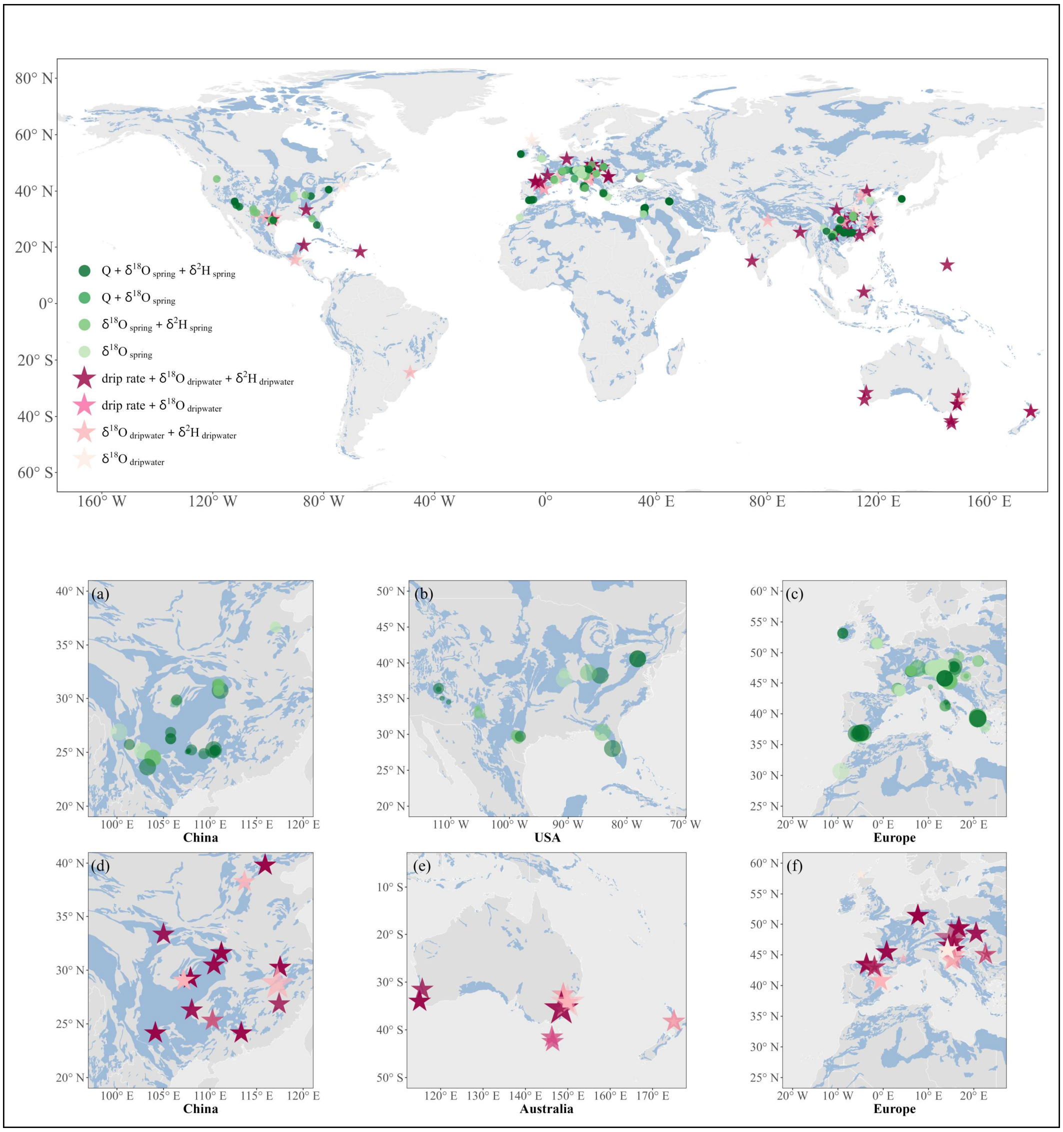

Figure 3: Geographic distribution of karst springs and cave sites included in the WoKaS-Iso database, along with the types of data available at each site. Blue areas indicate karst regions from the World Karst Aquifer Map (WOKAM, Chen et al. 2017). "Q" in the legend refers to

https://doi.org/10.5194/essd-2025-812
Preprint. Discussion started: 15 January 2026

karst spring discharge. ‘Green round’ symbols represent karst springs; ‘red star’ symbols represent caves. The symbol color intensity reflects the richness of available data combinations at each site, categorized into four subgroups: **flow rate+ δ¹⁸O+ δ²H**, **flow rate+ δ¹⁸O, δ¹⁸O+ δ²H, δ¹⁸O**, with darker color indicating more comprehensive datasets including both hydrological and isotopic data. Panels (a), (b), and (c) show zoomed-in maps of karst springs in China, the USA, and Europe, respectively. Panels (d), (e), and (f) show zoomed-in maps of cave sites in China, Australia, and Europe. In the zoomed maps, the size of each symbol presents the sampling resolution of δ¹⁸O and δ²H time series at each spring and cave drip site. The temporal resolution is categorized into three classes: **less than biweekly, monthly and coarser than monthly**, corresponding to large, medium and small markers respectively.

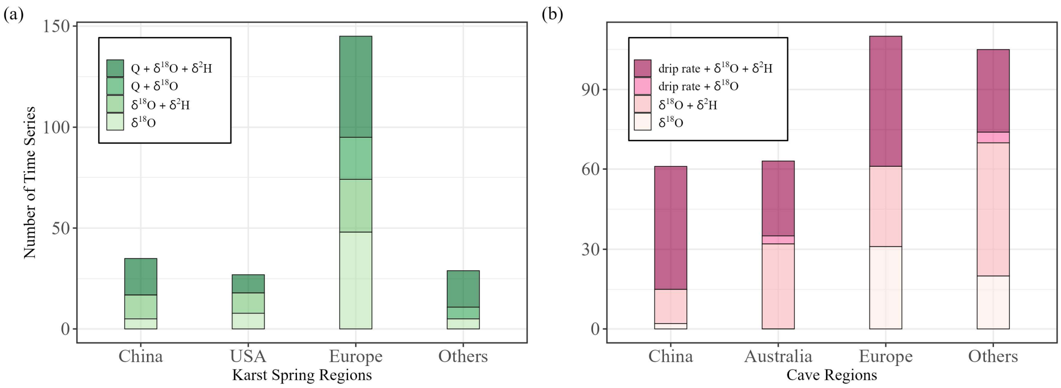

Figure 4: Summaries of data types across the major karst regions for (a) karst springs and (b) cave drip water sites. In panel (a), “Q” in the legend represents karst spring discharge.

Stable isotopes in spring discharge and drip waters can show strong seasonal variability due to fluctuations in precipitation, and temperature under changing climatic conditions. Adequate temporal resolutions are necessary to quantify these seasonal dynamics in detail and capture short-term hydrological patterns during rainfall or snowmelt events. Information about the temporal resolution of the available datasets is given in the regional maps in Figs 3a-f. For karst springs, Figs 3abc indicate that the sampling interval at most springs in China was at a monthly time scale. The resolution of springs in the USA is distributed evenly at monthly to coarser resolution. In Europe, 52 springs were monitored at a resolution of less than biweekly and 67 springs were visited at monthly resolution; only a small part of springs have coarser resolution. For the cave drip sites (Figs 3def), there are 90% cave drip isotopes at monthly sampling intervals in China, 56% in Australia as well as 70% in Europe. In contrast, the percentage of finer than biweekly is lower than 6% in any of three targeted regions.

A general overview of available temporal resolution is provided in Fig.5. Nearly 50% of spring discharge datasets have a high resolution of finer than daily, and over 12% cave drip rate datasets situated in the same class (Fig 5a). The dominant resolution of cave drip rate falls between biweekly and monthly, reaching around 74%, whereas the resolutions of spring discharge datasets are more evenly spread across four categorized resolution classes. However, a noticeable portion of spring discharge datasets exceed the monthly interval. For the stable isotope records from springs and cave drips, the primary resolution is

https://doi.org/10.5194/essd-2025-812
Preprint. Discussion started: 15 January 2026

Open Access Earth System Science Data Discussions

within biweekly-to-monthly range, accounting for around 64% of cave drip isotope datasets and over 40 % of spring data. Furthermore, 36% of isotope datasets from karst springs were measured at a resolution finer than biweekly. For cave drip sites, 27 % records were sampled at the coarser-monthly interval.

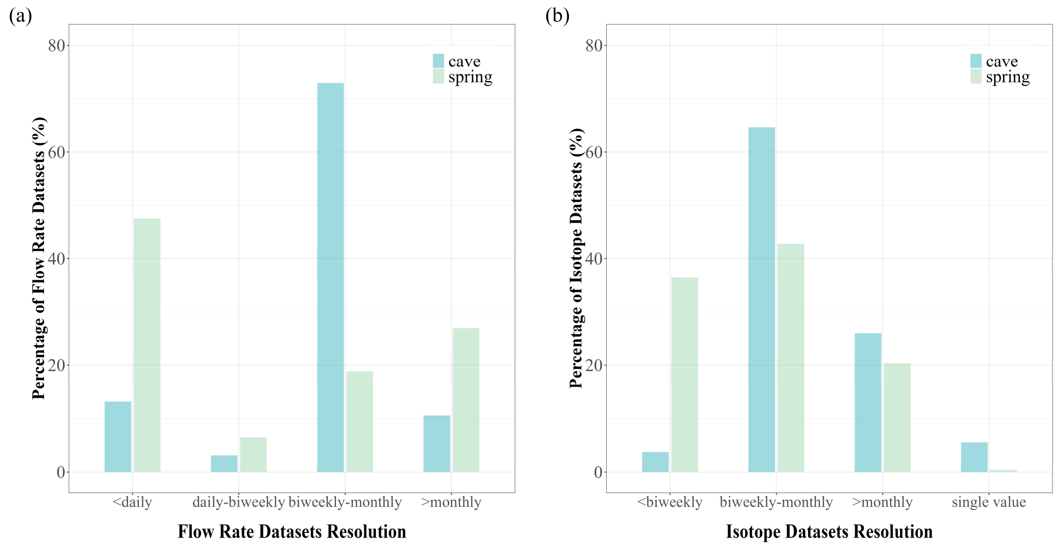

Figure 5: (a) Proportions of temporal resolution categories of discharge and drip rate datasets for karst springs and cave drip sites; The datasets are divided into four resolution levels: **finer than daily, daily to biweekly, biweekly to monthly** and **coarser than monthly**. (b) Proportions of temporal resolution categories of stable isotopes for karst springs and caves. The resolutions are stratified into four categories: **finer than biweekly, biweekly to monthly, coarser than monthly** and **single-value records.**

2.2 System input data

2.2.1 Available data types

The WoKaS-Iso database includes the precipitation amount and precipitation $\delta^{18}O$ and $\delta^{2}H$ observations for karst springs and cave sites, compiled from the same sources described in subsection 2.1.2 (also see Table 1 & Figure 2). To ensure adequate spatial and temporal coverage, karst springs and cave sites lacking local rainfall and rainwater isotopes records were supplemented with the data from Global Network of Isotopes in Precipitation (GNIP) database. Firstly, the geographic coordinates of karst springs, cave sites, and GNIP stations within the related countries were imported into ArcGIS where the closest GNIP station to each karst spring and cave site was identified. Secondly, the distances between the springs or caves and their nearest GNIP stations were measured using ArcGIS. With the aim of reflecting representative of the local climatic and isotopic characteristics for karst springs and caves, only GNIP stations within 25 km were retained.

https://doi.org/10.5194/essd-2025-812
Preprint. Discussion started: 15 January 2026

For karst springs, 20 sites possess local rainfall measurements, and 99 springs derive precipitation data from nearby meteorological stations including GNIP stations, while the remaining 117 springs lack rainfall data. Regarding precipitation isotope observations, only 18 springs are with auxiliary local isotope data, 104 springs use the data from meteorological or GNIP network, and 114 springs have no related isotope records. For cave sites, 21 caves include locally measured rainfall, 37 caves obtained rainfall data from adjacent weather stations, and 16 caves without rainfall records. As for precipitation isotopes, 33 caves are associated with local measurements, 33 caves rely on weather stations-based isotope datasets or GNIP-derived data, and 8 caves lack isotope observations. To offer comprehensive metadata for input observations, the distance from the precipitation and precipitation isotopes sampling sites to cave/spring sites were calculated where geographic coordinates were available, documented in the metadata tables for spring input and cave input datasets.

Since datasets on precipitation amount and precipitation $\delta^{18}O$ and $\delta^{2}H$, observed locally or provided by GNIP, were not available at all or output locations or limited in their temporal extent, the WoKaS-Iso database includes complementary datasets from six global products for continuous rainfall, precipitation $\delta^{18}O$ and $\delta^{2}H$, air temperature as well as both actual and potential evapotranspiration. The information of these global products used in this study are listed in Table 2, including relevant modelled variables, time span, spatial and temporal resolution and the source for the construction of models.

Precipitation data were obtained from MSWEP v2.8 (Beck et al., 2017, 2019a, b), a multi-source ensemble product offering daily and monthly estimates at 0.1° resolution from 1979–2020. MSWEP improves global precipitation accuracy by combining gauge, satellite, and reanalysis data using a weighted ensemble based on network density and local performance (Liu et al., 2019). Evaporation estimates were sourced from GLEAM v4.1a (Hulsman et al., 2023; Koppa et al., 2022; Martens et al., 2017; Miralles et al., 2011, 2025; Zhong et al., 2022), which integrates satellite data and physical modelling with machine learning to estimate daily and monthly actual and potential evaporation at 0.1° resolution from 1980–2023. Air temperature time series were extracted from ERA5, the fifth-generation atmospheric reanalysis developed by ECMWF (Hersbach et al., 2020, 2023), which provides consistent daily climate data since 1940 at 0.25° resolution using 4D-Var data assimilation technique and the CY41R2 forecasting system. To characterize precipitation isotope variability, we used monthly $\delta^{18}O$ and $\delta^{2}H$ outputs from IsoGSM (Kanamitsu et al., 2002; Nan et al., 2021; Yoshimura et al., 2008), a general circulation model incorporating isotopic fractionation and nudged with NCEP (National Centres for Environmental Prediction) reanalysis data, covering 1979–2021. Additionally, long-term spatial isotope patterns were derived from the Isoscape product (etopo5, 2025; Bowen et al., 2005; Bowen and Revenaugh, 2003; Bowen and Wilkinson, 2002), which interpolates GNIP data using topographic and geographic predictors at a 5-arcminute resolution. Finally, seasonal isotope dynamics were represented using the sinusoidal precipitation isotope model (Allen et al., 2019), which fits annual sine curves to global precipitation isotope records and maps the resulting parameters to derive daily and monthly isotope predictions from 60°S to 90°N. Together, these products provide a consistent climatological and isotopic framework for interpreting site-level karst and cave hydrology.

https://doi.org/10.5194/essd-2025-812
Preprint. Discussion started: 15 January 2026

Open Access Earth System Science Data Discussions

Table 2: Information of the global products included in the WoKas_Iso database

Variable	Model Name	Data Source	Spatial Resolution	Temporal Resolution	Spatial Coverage	Time Coverage	Reference
Precipitation	MSWEP[1]v2.8	Gauge, Satellite, Reanalysis	0.1°	Daily/Monthly	Global	1979–2020	(Beck et al., 2019b)
Precipitation isotopes	IsoGSM[2]	Reanalysis	200 km	Monthly	Global	1979–2021	(Yoshimura et al., 2008)
Precipitation isotopes	Isoscape	GNIP[4]	5 arcmin	Monthly	Global	Jan–Dec	(Bowen et al., 2005)
Precipitation isotopes	Sine Curve	GNIP, CNIP[5], USNIP[6]	5 arcmin	Daily/Monthly	60°S–90°N	Jan–Dec	(Allen et al., 2019)
Air temperature	ERA 5	Reanalysis	31 km	Daily/Monthly	Global	1940–2024	(Hersbach et al., 2023)
Evapotranspiration	GLEAM[3] 4.1a	Satellite, Reanalysis	0.1°	Daily/Monthly	Global	1980–2023	(Miralles et al., 2025)

[1]Multi-Source Weighted-Ensemble Precipitation
[2]Isotopes-integrated Global Spectral Model
[3]Global Land Evaporation Amsterdam Model
[4]Global Network of Isotopes in Precipitation
[5]Canadian Network for Isotopes in Precipitation
[6]US Network for Isotopes in Precipitation

2.2.2 Evaluation of different precipitation isotope data

While global precipitation and evapotranspiration data were evaluated with observations in their original studies (see Table 2), an evaluation of the isotopic composition of rainfall provided by the three precipitation isotope models—IsoGSM, Isoscape, and the Sine Curve model, is still required. For that, we compared monthly simulated precipitation $\delta^{18}O$ and $\delta^{2}H$ against site-specific observations from both cave drip water and karst spring locations. For precipitation $\delta^{18}O$ comparison, a total of 55

https://doi.org/10.5194/essd-2025-812
Preprint. Discussion started: 15 January 2026

Open Access Earth System Science Data Discussions

sites were analysed comprising 26 cave locations,15 spring locations and 14 nearby meteorological stations to compensate the limited availability of isotopic measurements at spring locations. For sites with daily precipitation, the monthly amount-weighted precipitation isotopes were calculated, while for sites lacking daily precipitation, the stepwise interpolation of precipitation isotopes was applied to derive monthly means. The same analysis was done for δ^2H (provided in supplement section S2).

We quantified the agreement of the global products and the observed isotopic composition of precipitation by the root-mean-square error (RMSE) and the coefficient of determination (R^2). Fig.6 presents the performance metrics in predicting δ^{18}O. Based on RMSE, IsoGSM displays the lower median RMSE value (~ 2 ‰) with a narrow interquartile and minimum outliers, indicating the most consistent predictions across both caves and springs. The Isoscape model exhibits a comparable median RMSE, though with a greater variability and higher outliers, reflecting less robustness. In contrast, the Sine Curve model yields the highest median error (>3‰) and broader distributions, highlighting significantly inferior performance. Concerning R^2, IsoGSM achieves the highest median R^2 (~0.6), however, its R^2 values span a wide range. The Isoscape model, having a slightly lower median R^2 value (~0.5), shows a tighter distribution. The Sine Curve model performs worst, with median R^2 less than 0.2 and a concentration of low values, indicating poor explanatory power.

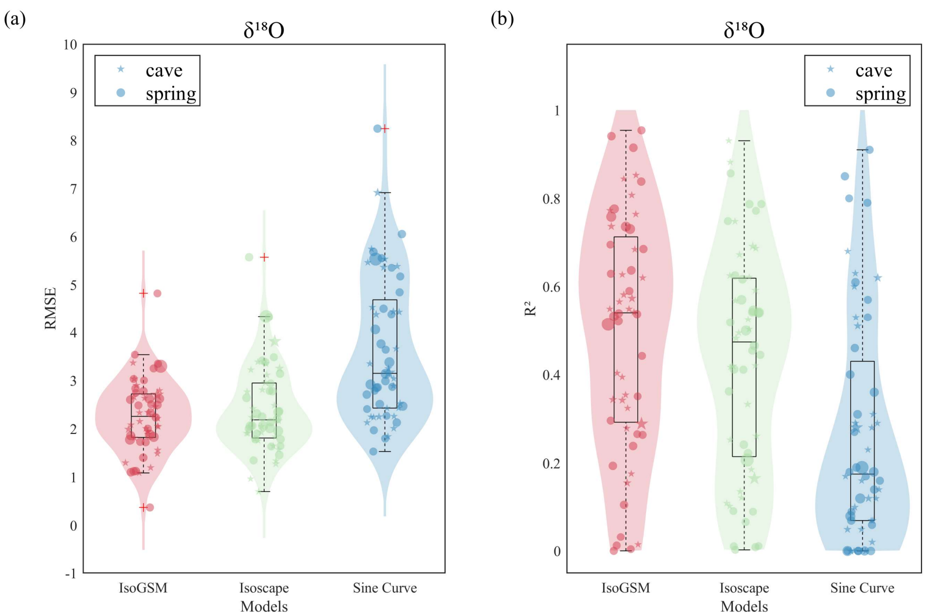

Figure 6: Statistical comparison of three model performance for δ^{18}O in precipitation at cave (stars) and springs sites (circles). (a) Root Mean Square Error (RMSE); (b) Coefficient of determination (R^2). Violin plots show the distribution of performance metrics for each model:

https://doi.org/10.5194/essd-2025-812
Preprint. Discussion started: 15 January 2026

Open Access Earth System Science Data Discussions

IsoGSM (red), Isoscape (green), and Sine Curve (blue). Boxplots within violin indicate the median, interquartile range and outliers. Lower RMSE and higher R^2 indicate better model performance.

To evaluate the different performances of the global datasets, we compare time series of observed monthly $\delta^{18}O$ and δ^2H with model outputs from the Sine Curve, IsoGSM, and Isoscape models across all selected locations. Fig. 7 shows the $\delta^{18}O$ comparisons at four representative sites: Liangfeng Cave, Yongxing Cave, Chaoshuidong Spring and the Met-II.uz meteorological station near Anyak Spring (see supplement Section S1 for a complete comparison for other 51 sites). Overall, the Sine Curve model shows limited ability in reproducing the temporal course of the observations. In contrast, the IsoGSM model closely aligns the observed $\delta^{18}O$ dynamics at four sites, yielding high R^2 values (0.85, 0.81, 0.94 and 0.78 for Liangfeng Cave, Yongxing Cave, Chaoshuidong Spring and the Met-II.uz meteorological station near Anyak Spring, respectively) alongside relatively low RMSE values, which reflects robust performance in both correlation and prediction accuracy. The Isoscape model attains moderate predictions with R^2 exceeding 0.5 at all four sites. Although it outperforms the Sine Curve model, it tends to be less reliable than IsoGSM in capturing the isotopic variability. A similar comparison is also performed for δ^2H (see supplement section S2) indicating similar performances of the global products with IsoGSM showing slightly superior performances over Isoscape and pronounced superior performance over the Sine Curve model. Different phase shifts between $\delta^{18}O$ and δ^2H in their Sine Curve model indicate a poor representation of their physical covariance which is given through the global/local meteoric waterline. Overall, IsoGSM provides the most accurate and robust $\delta^{18}O$ predictions, for which reason we recommend it for those cave and spring locations where no local observations are available.

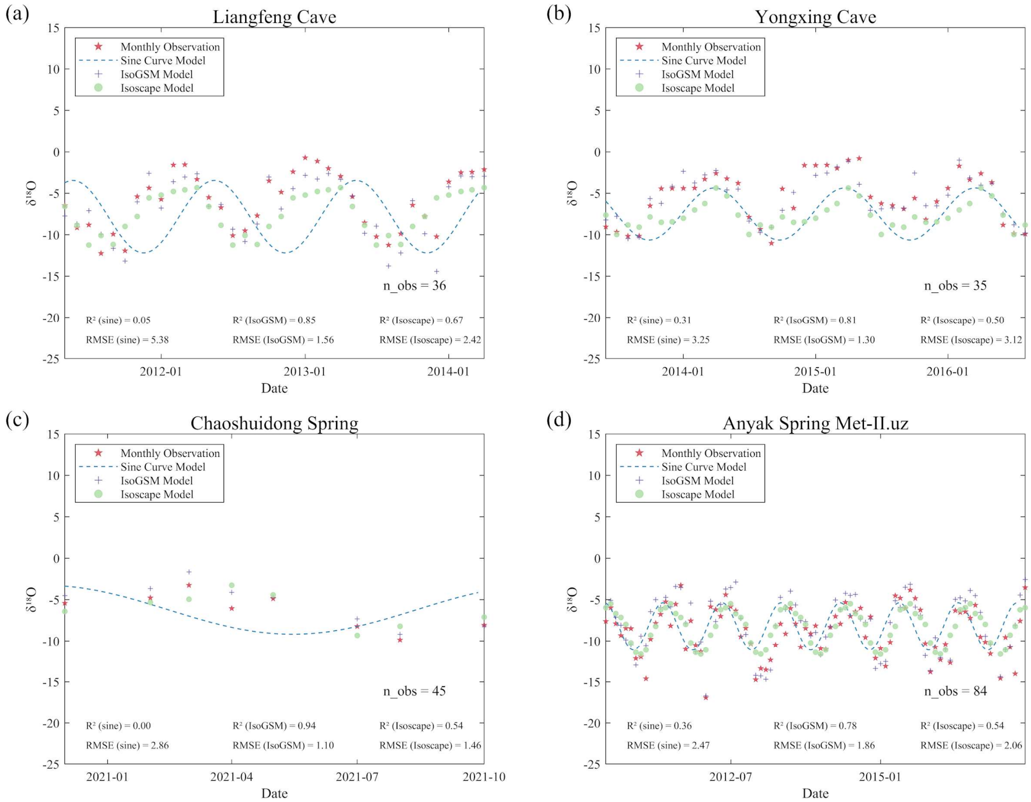

Figure 7: Time series comparison of modelled and observed monthly δ¹⁸O in precipitation at two cave sites (a–b) and two spring sites (c–d). Observations (red stars) are compared with estimates from the Sine Curve model (dashed blue line), IsoGSM (purple crosses), and the Isoscape model (green circles). Each panel shows the number of monthly observations (n.obs) and model performance statistics (R^2 and RMSE).

3 Database structure and usage notes

The datasets compiled in the WoKaS-Iso database are publicly archived as a zipped package titled "WoKaS_Iso_Data_Records" in OPARA, an open-access repository of research data from Saxon Universities (https://doi.org/10.25532/OPARA-909; Zang, 2025). The zip file is organized into three main folders: WoKaS_Iso_Input_Data, WoKaS_Iso_Output_Data, Global_Products_Data. Each folder is subdivided into several subfolders, with their structure and contents described in the following section:

https://doi.org/10.5194/essd-2025-812
Preprint. Discussion started: 15 January 2026

3.1 WoKaS_Iso_Input_Data

Contains precipitation amount and precipitation isotopes ($\delta^{18}O$ and δ^2H) metadata tables and corresponding datasets for karst springs and cave sites:

i. **WoKaS_Iso_Spring_Input_Metadata** provides summarised information on the precipitation and precipitation isotopes sites associated with each spring included in the database. Each spring is assigned a unique identifier as *wokas_iso_id*, which is constructed by using ISO country code (e.g., *AT* for Austria), a data type indicator (*S* for spring and *C* for cave) and a serial number (e.g., *AT-S-0001*). Some springs are associated with multiple precipitation or precipitation isotopes sites sharing the same *wokas_iso_id*, but each site is assigned its own *precipitation_entity_name* and *precip_iso_entity_name* as keys to link the metadata with their corresponding dataset. Furthermore, the *precip_distance_to_spring* and *precip_iso_distance_to_spring* indicate the distance in meters from each site to the specific spring. This structure allows users to flexibly select the desirable sites for their use. The full list of variables included in the spring input metadata table are explained in the Table 3.

ii. **WoKaS_Iso_Spring_Input_Datasets** consists of 135 csv files. Each csv file represents the time series of precipitation amount and precipitation $\delta^{18}O$ and δ^2H for a specific spring. The csv file naming format is *Input-wokas_iso_id@spring_name* (e.g., *Input-AT-S-0002@Wasseralmquelle(A)*). Each csv file contains *wokas_iso_id*, *precipitation_entity_name*, *date_precip* (precipitation observation date), *precipitation*, *unit* (precipitation amount unit), *precip_iso_entity_name*, *date_precip_iso* (precipitation isotopes sampling date), *d18O*, *dD* and *note*.

iii. **WoKaS_Iso_Cave_Input_Metadata** offers metadata summaries for cave sites input data, structured in the same way as the spring input metadata table. Similarly, each cave identifier is assigned to the cave site consisting of the ISO country code, the cave data type indicator *C* and its serial number (e.g., *AT-C-0001*). The entity name and distance fields align with the same conventions as springs. All variables are consistent with those used for spring metadata and are presented in Table 3.

iv. **WoKaS_Iso_Cave_Input_Datasets** contains 67 csv files; each refers to a specific cave site. The csv file naming convention and internal structure follow the same pattern (e.g, *Input-AT-C-0001@Obir Cave*) as described in the spring input datasets section.

Table 3: Description of variables in the spring/cave input data metadata files

Variable	Description	Variable	Description
country	country the spring /cave is in	precip_iso_distance_to_spring/cave (m)	distance between precipitation isotope site and spring/cave (m)
wokas_iso_id	WoKaS-Iso identifier	precip_iso_enetity_name	identifier assigned to precipitation isotopes site linked to a specific spring/cave
sisal_monv1_id/wokas_id	cave/spring identifier in SISAL_monv1/WoKaS database	precip_iso_latitude	precipitation isotopes measurements site latitude in decimal degrees. (N+, S-)

https://doi.org/10.5194/essd-2025-812
Preprint. Discussion started: 15 January 2026

Open Access Earth System Science Data Discussions

spring/cave_name	spring/cave name	precip_iso_longitude	precipitation isotopes measurements site longitude in decimal degrees. (E+, W-)
precipitation_site_name	location of precipitation measurements	precip_iso_elevation	meters above mean sea level
precip_distance_to_spring/cave(m)	distance between precipitation site and spring/cave	precip_d18O_start_date	start day of the oxygen-18 measurement in rainwater sample(dd/mm/yyyy)
precip_entity_name	identifier assigned to precipitation site linked to a specific spring/cave	precip_d18O_end_date	end day of the oxygen-18 measurement in rainwater sample(dd/mm/yyyy)
precip_latitude	P site latitude in decimal degrees. (N+, S-)	precip_d18O_observation_length	number of oxygen-18 measurements in rainwater
precip_longitude	P site longitude in decimal degrees. (E+, W-)	precip_dD_start_date	start day of the deuterium measurement in rainwater sample(dd/mm/yyyy)
precip_elevation	meters above mean sea level	precip_dD_end_date	end day of the deuterium measurement in rainwater sample(dd/mm/yyyy)
precipitation_start_date	start day of precipitation measurement(dd/mm/yyyy)	precip_dD_obeservation_length	number of deuterium measurements in rainwater
precipitation_end_date	end day of precipitation measurement(dd/mm/yyyy)	precip_iso_data_source	isotopic datasets in precipitation from who or where
precip_observation_length	number of precipitation measurements	reference	relevant literatures
precip_data_source	precipitation datasets from who or where	additional information	free-text column
precip_isotopes_site_name	location of precipitation Isotopes measurements		

3.2 WoKaS_Iso_Output_Data

Includes output metadata tables and output datasets for karst springs and cave drip sites:

i. **WoKaS_Iso_Spring_Output_Metadata** summarizes attributes for karst springs documented in the WoKaS-Iso database including the geographic information of springs, an overview of karst spring discharge and isotopes for each spring. Each spring has the consistent identification through unique *wokas_iso_id*, same identifier used in the spring input data records. In the same way, the specific fields *discharge_entity_name* and *isotope_entity_name* are designed to establish the connection to their corresponding datasets. The complete list of parameters contained in the spring output metadata table are shown in Table 4.

https://doi.org/10.5194/essd-2025-812
Preprint. Discussion started: 15 January 2026

ii. **WoKaS_Iso_Spring_Output_Datasets** presents karst spring discharge, $\delta^{18}O$ and/or $\delta^{2}H$ datasets for 236 springs, organized as separate 236 csv files. Every csv file follows a standardized naming format "*Output-wokas_iso_id@spring_name*" (e.g., *Output-AT-S-0002@Wasseralmquelle(A)*). The uniform internal structure of workbook includes the following columns: *wokas_iso_id*, *discharge_entity_name*, *date_discharge* (measurements date), *discharge*, *discharge_unit* (the unit of discharge), *iso_entity_name*, *date_iso* (isotope data sampling date), *d18O* and *dD*.

Table 4: Description of variables in the spring output metadata table

Variable	Description	Variable	Description
country	country the spring is in	discharge_data_source	spring discharge datasets from who or where
wokas_iso_id	WoKaS-Iso identifier	isotope_entity_name	identifier assigned to link the metadata to its isotopic datasets
wokas_id	spring identifier in WoKaS database	d18O_start_date	start day of oxygen-18 data collection of spring water sample(dd/mm/yyyy)
spring_name	spring name	d18O_end_date	end day of oxygen-18 data collection of spring water sample(dd/mm/yyyy)
latitude	spring latitude in decimal degrees. (N+, S-)	d18O_observation_length	number of oxygen-18 measurements
longitude	spring longitude in decimal degrees. (E+, W-)	d2H_start_date	start day of deuterium data collection of spring water sample(dd/mm/yyyy)
elevation(m)	meters above mean sea level	d2H_end_date	end day of deuterium data collection of spring water sample(dd/mm/yyyy)
type	spring	d2H_observation_length	number of deuterium measurements
discharge_entity_name	identifier assigned to link the metadata to its discharge datasets	isotope_data_source	spring isotopic datasets from who or where
discharge_start_date	start day of spring discharge measurement(dd/mm/yyyy)	reference	relevant literatures
discharge_end_date	end day of spring discharge measurement(dd/mm/yyyy)	additional_information	free-text column
discharge_observation_length	number of spring discharge observations		

iii. **WoKaS_Iso_Cave_Output_Metadata** comprises a comprehensive overview of cave drip rate and cave drip isotopic records ($\delta^{18}O$ and $\delta^{2}H$) for all cave drip sites. Each cave includes multiple drip sites which are assigned the same *wokas_iso_id* which is assigned in the cave input section but are distinguished by the unique *drip_rate_entity_name* and *drip_iso_entity_name* entries. Explanations for each variable in the cave output meta table is presented in Table 5.

iv. **WoKaS_Iso_Cave_Output_Datasets** contains 73 csv files. Each csv file stores the drip rate and drip isotopes datasets for the individual cave. The csv file name follows the format *Output-wokas_iso_id@cave_name* (e.g., *Output-AT-C-0001@Obir Cave*). Within each csv, multiple drip sites are documented using their unique entity names. The content includes the columns: *wokas_iso_id*, *drip_rate_entity_name*, *date_rate* (drip rate measurement date), *unit* (the unit of drip rate), *drip_iso_entity_name*, *date_iso* (sampling date of drip water isotopes), *d18O* and *dD*.

Table 5: Description of variables in the cave output metadata table

Variable	Description	Variable	Description
country	where the spring is located	drip_rate_observation_length	number of cave drip rate observations
wokas_iso_id	WoKaS-Iso identifier	drip_isotopes_entity_name	assigned identifier to link the metadata to related drip water isotopic data
sisal_monv1_id	cave identifier in SISAL_monv1database	drip_d18O_start_date	start day of oxygen-18 data collection of drip water sample(dd/mm/yyyy)
name	cave name	drip_d18O_end_date	end day of oxygen-18 data collection of drip water sample(dd/mm/yyyy)
latitude	cave latitude in decimal degrees. (N+, S-)	drip_d18O_observation_length	number of drip oxygen-18 measurements
longitude	cave longitude in decimal degrees. (E+, W-)	drip_d2H_start_date	start day of deuterium data collection of drip water sample(dd/mm/yyyy)
elevation(m)	meters above mean sea level	drip_d2H_end_date	end day of deuterium data collection of drip water sample(dd/mm/yyyy)
type	cave	drip_d2H_observation_length	number of drip deuterium measurements
drip_site	cave drip site name	data_source	drip rate and drip isotopes datasets from where or who
drip _rate_entity_name	assigned identifier to link the metadata to related drip rate data	reference	relevant literatures
drip_rate_start_date	start day of cave drip rate measurement(dd/mm/yyyy)	additional_information	free-text column
drip_rate_end_date	end day of cave drip rate measurement(dd/mm/yyyy)		

https://doi.org/10.5194/essd-2025-812
Preprint. Discussion started: 15 January 2026

Open Access Earth System Science Data Discussions

3.3 Global_Products_Data

Contains gridded datasets from six global models. Each product has a dedicated folder with its name WoKaS_Iso_MSWEP, WoKaS_Iso_GLEAM, WoKaS_Iso_ERA5, WoKaS_Iso_IsoGSM, WoKaS_Iso_Isoscape, WoKaS_Iso_Sine_Curve, WoKaS_Iso_Scripts.

- WoKaS_Iso_MSWEP, WoKaS_Iso_GLEAM, WoKaS_Iso_ERA5, WoKaS_Iso_Sine_Curve: the modelled data from these products are systematically sorted into four subfolders according to location type (spring or cave) and time resolution (daily or monthly). For example, WokaS_Iso_MSWEP folder includes WoKaS_Iso_Daily_MSWEP_Caves, WoKaS_Iso_Daily_MSWEP_Springs, WoKaS_Iso_Monthly_MSWEP_Caves, WoKaS_Iso_Monthly_MSWEP_Springs. Each subfolder contains compatible csv files storing continuous time series for individual spring or cave. The csv file names adhere to a standardized naming rule, combining the product name, temporal resolution, the *wokas_iso_id* and spring /*cave name*. For instance, *MSWEP_Daily_AT-C-0001@Obir Cave* refers to the daily gridded datasets from MSWEP at Obir Cave in Austria.
- WoKaS_Iso_IsoGSM, WoKaS_Iso_Isoscape: Since IsoGSM and Isoscape provide monthly $\delta^{18}O$ and $\delta^{2}H$ data only, each folder is subdivided into two categories for caves and springs: WoKaS_Iso_IsoGSM/Isoscape_Monthly_Caves and WoKaS_Iso_IsoGSM/Isoscape_Monthly_Springs. While, the csv file naming is slightly different from other products, constructed using *IsoGSM/Isoscape_wokas_iso_id@spring/cave_name* (e.g., *IsoGSM_AT-C-0001@Obir Cave; Isoscape_AT_C_0001@Obir Cave*).
- WoKaS_Iso_Scripts: this folder includes three MATLAB scripts developed to aid users in extracting daily and monthly data from NetCDF files of MSWEP, GLEAM and ERA5. The accompanying README file offers detailed instruction on how to use the scripts and the download guidelines for each product, which assists users efficiently integrate authoritative gridded datasets into their workflows.

3.4 Usage notes

- **Metadata:** The columns *precip_data_source*, *precip_iso_data_source* (in the spring and cave input meta tables), *discharge_data_source*, *isotope_data_source* (in the spring output meta table), *data_source* (in the cave output meta table) specify the origins of respective data: precipitation, precipitation isotopes, discharge, spring isotopic data, cave drip rate and cave drip isotopes respectively. These sources can include data contributors, or digitization from specific figures or tables in publications, reports or theses, or retrieval from online repositories with links provided if applicable. All meta tables include the *reference* column listing all related literature that:(1) the spring/cave drip site was studied; (2) the data were originally published; (3) contained figures and tables were digitized. These references enable users to get further context regarding datasets sampling method, climate conditions, hydrogeological settings of the studied spring/cave system. For peer-reviewed publications, DOIs are offered, while URLs of reports or theses are provided if available.

https://doi.org/10.5194/essd-2025-812
Preprint. Discussion started: 15 January 2026

- **Machine-readability:** All csv files storing input and output datasets are designed in a machine-readable format to facilitate efficient and automated data processing.
- **Link the metadata to datasets:** Each csv file name incorporates the unique *wokas_iso_id* that is organized in the metadata tables. This identifier enables location of the related spring or cave dataset by matching with file name (e.g. *Output-wokas_iso_id@spring_name*). Additionally, within each csv file, the entity name fields (*precip_entity_name*, *precip_iso_entity_name*, *discharge_entity_name*, *isotope_entity_name*, *drip_rate_entity_name* and *drip_iso_entity_name*) can work as the identified keys to connect with the corresponding metadata entries. These identifiers can be utilized to retrieve specific time series data from the measurement sites of interest.
- **Global products datasets:** Model-derived data corresponding to each site are provided in CSV files named according to their respective wokas_iso_id for easy reference. Monthly datasets, dates are separated into two columns: year and month, while daily data use a single dd/mm/yyyy format. These data represent the closest grid cell to each site; therefore, users should be aware of potential spatial differences when comparing with local observations. Proper citation of original data sources is required when utilizing these datasets.
- **Global products scripts:** The provided scripts are designed to extract data at monthly and daily resolutions from the MSWEP, GLEAM, and ERA5 datasets, corresponding to the time periods listed in Table 2. Users can apply these scripts to extract data at any geographic coordinates of interest. The global product data correspond to the grid cell closest to the site coordinates. Users should be aware of potential spatial mismatches. Automated data download routines are not included; instructions for obtaining the required NetCDF files are provided in the accompanying README file.

4 Data quality control and evaluation

4.1 Data quality control

A series of quality control measures were implemented throughout the large datasets synthesized in the WoKaS-Iso database to ensure data precision, consistency and integrity:

Site information verification: All spring and cave drip site names, coordinates, elevation, data units, precipitation sites and precipitation isotope sampling sites were initially cross-checked against the original sources: supplementary materials, tables, original data contributed by collaborators or digitized from related figures. Additionally, all the time series were reviewed for consistency with the original datasets, ensuring correct sampling date accurately matching its associated measurements to avoid any discrepancies.

Standardized formatting:

i. Naming convention: All *wokas_iso_id* entries were validated to confirm conformity with the standardized naming convention including verification of the ISO country code, data type indicator (C for cave and S for spring) and

https://doi.org/10.5194/essd-2025-812
Preprint. Discussion started: 15 January 2026

sequential numbering within each country. The csv file names were systematically reviewed folder by folder to ensure compliance with the naming patterns stated in section 3.

ii. CSV file structure: All files were checked to be machine-readable in comma-delimited csv format. Each csv file was examined to guarantee a consistent internal structure with uniform column headers.

iii. Date and coordinates formatting: The dates were formatted consistently in dd/mm/yyyy across all datasets. The latitude and longitude were formatted with four decimals.

Consistency checks:

i. Data consistency: The dates and corresponding time series of all datasets were checked to confirm they were sorted chronologically.

ii. Spatial consistency: Latitude and longitude were validated to fall in valid ranges (N+, S-, E+, W-), and validation of spatial distribution on map were verified by visualization.

iii. Metadata and datasets matching: The identifiers *wokas_iso_id*, *precip_entity_name*, *precip_iso_entity_name*, *discharge_entity_name*, *iso_entity_name*, *drip_rate_entity_name* and *drip_iso_entity_name* were cross validated against metadata to ensure correct linkage with the corresponding datasets. In addition, the start date, end date and observation length of all time series were checked to align with actual datasets.

Data source verification: Checking data sources recorded in the meta tables was implemented to ensure proper citation and traceability. The indicated figures and tables were checked to be correctly represented. All provided URLs access to online database were tested to verify datasets retrieval. The DOIs (provided as web links) were confirmed working and accurately linked to the cited publications. Where available, links of reports and theses were also tested for accessibility.

For cave drip water datasets originating from SISAL_mon_v1, WoKaS-Iso builds on the automated quality control already applied in Treble et al. (to be submitted). Within WoKaS-Iso quality control, the SISAL_mon_v1 records were therefore not re-processed from scratch, but underwent additional harmonisation and validation steps: mapping to the WoKaS-Iso file and naming conventions, cross-checking identifiers and time ranges against the new metadata structure, and ensuring consistent linkage and interoperability with associated precipitation and spring datasets and references as described in the following.

4.2 Data quality attribution

The datasets quality for each spring and cave site was assessed based on an attribution scheme assigning scores to both output and input data according to their sources (Table 6). For output data, **collected spring discharge/drip rate** and **collected spring/drip water isotope** were obtained from research collaborators, original authors, online databases or supplementary materials of publications. These sources are generally of high quality and were hence assigned a score of 3. **digitized spring discharge/drip rate** and **digitized spring/drip water isotope** were digitized from the plots in publications or reports or theses. Although the extraction process was carried out as precisely as possible, some inaccuracies and uncertainties inherently remained due to the resolution and temporal coverage of the original plots. Thus, the score of 2 was assigned to the digitized data. For those locations without relevant data were given a score of 0. For input data, three quality levels were defined

https://doi.org/10.5194/essd-2025-812
Preprint. Discussion started: 15 January 2026

according to the sources of precipitation isotopes and precipitation information: local measurements, meteorological stations and global models. The **local observation (precip. isotope/amount)** acquired from on-site monitoring, which are rare and valuable particularly for karst springs, were thus assigned the highest score of 3. The **meteorological stations (precip.isotope/amount)** data sourced from meteorological stations, while still based on measurements, are deemed less directly representative of site-specific conditions and were scored 2. In cases where neither local nor station-based input were available, the input data from **Global products** were provided as substitutes and assigned a score of 1. The total grade for each spring and cave site was calculated from the sum of its output and input data scores, based on the assessment criteria stated above. The sites evaluation was then divided into three classes that reflect the overall reliability and completeness of the data collection.

- **Class I** (scores from 10 to 12): indicating robust datasets with high quality, generally obtained from raw output origins and/or locally measured inputs. The site in this category keeps the most complete and reliable datasets, providing comprehensive information for interpretation and modelling of karst systems.
- **Class II** (scores from 7 to 9): reflecting the datasets with moderate quality that might have less site-specific input sources or digitized outputs. Although less strong, these data are still valuable for studies in both karst geohydrology and speleology.
- **Class III** (scores below 7).: the sites with lower-confidence data, primarily relying on digitized records or global modelled data. These datasets are helpful in identifying data-scarce regions and highlighting the need for more data collection.

Table 6: The grading system for evaluation of the WoKaS-Iso database for karst springs and caves. *Example:* a spring with collected spring discharge (3 points), collected spring isotopes (3 points), local observation of precipitation isotopes (3 points), and local precipitation amount (3 points) receives a total score of 12. *Note:* the "*No data*" category is assigned to sites without flow rate data or aligned with SISAL_mon_v1 database at Shenqi Cave, as no cave drip water data are available and only input data are provided.

System output data		**System input data**	
Variable	Assigned Score	Variable	Assigned Score
Collected spring discharge/drip rate Collected spring /drip water isotope	3	Local observation (precip. isotope/amount)	3
Digitized spring discharge/drip rate Digitized spring/drip water isotope	2	Meteorological stations (precip.isotope/amount)	2
No data	0	Global products	1

https://doi.org/10.5194/essd-2025-812
Preprint. Discussion started: 15 January 2026

Attributing the quality classes to all our sites shows that most of them fall within Class I and Class II (Figure 8). For springs, 21% are categorized into Class I, and are predominantly distributed in China, Europe and the Middle East. Class II springs, the most common category, occupied 47%, due to scarcity and limited availability of locally measured rainfall and rainwater isotopes for karst springs; while Class III accounts for 32%, with a high proportion due to the absence of paired precipitation and precipitation isotopes measurements for karst springs, the substitute modelled data were used. Class I and Class II are spread relatively evenly globally, while Class III springs are primarily found in Europe where karst spring monitoring is more extensive in the WoKaS-Iso database. For cave sites, a high proportion of 50% is classified as Class I, Class II reached 46%, with only a small proportion of 4% falling into Class III. The distribution characteristics reflect the more complete and robust monitoring systems available for caves compared to karst springs. The Class I cave sites are mainly suited in Australia, China and Europe. The Class II caves are mostly located in Europe and the USA. Only 4 caves are grouped as Class III, scattered over various regions.

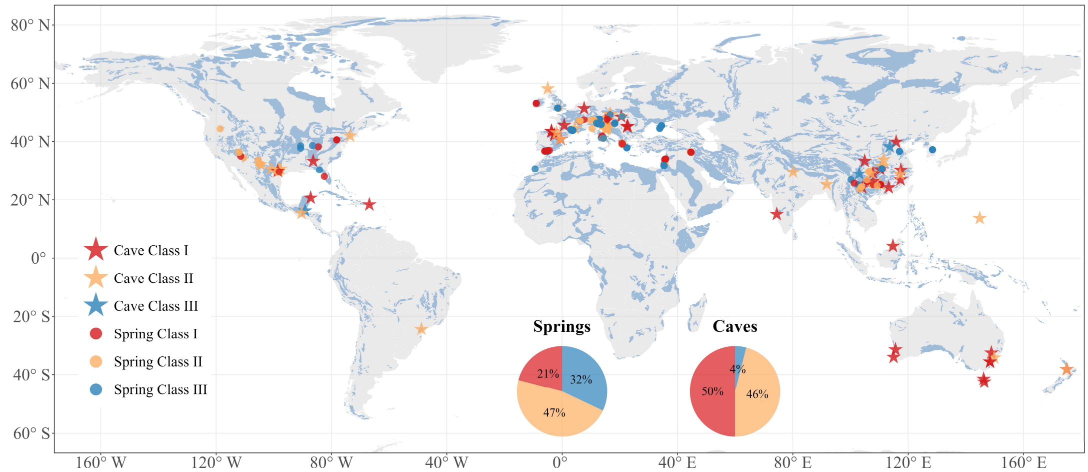

Figure 8: Spatial distribution of karst springs and cave sites in the WoKaS_Iso database according to data quality evaluation classes. Blue areas indicate karst regions as delineated in the World Karst Aquifer Map (WOKAM, Chen et al., 2017). Star symbols refer to caves and circle symbols represent springs. Colours represent the three quality tiers: Class I (red), Class II (orange), and Class III (blue). Accompanying pie charts illustrate the proportion of each quality class for springs and caves, respectively.

https://doi.org/10.5194/essd-2025-812
Preprint. Discussion started: 15 January 2026

Open Access Earth System Science Data Discussions

5 Data availability

The dataset is available in the public repository at: https://doi.org/10.25532/OPARA-909 (Zang, 2025).

6 Recommended usage and outlook

The data quality classification provides guidance for users on the proper application and interpretation of each site. **Class I** with the most complete observational records are recommended for process-based model calibration and validation, characterization of the karst system and paleoclimate construction**. Class II** consisting of partial measurements or digitized output data or station-based input data/ modelled sources are appropriate for regional-scale comparative studies, trend analysis and model sensitivity testing. Although less precise than Class I, these datasets remain valuable in regions with limited monitoring. **Class III**, which rely highly on digitised outputs and global products inputs, are useful for global exploratory studies, particularly in data-scarce regions. Global products offer critical alternatives where observations are unavailable and support long-term climate analysis. Based on our analysis, we recommend **IsoGSM** as the preferred substitute of precipitation isotope input. Future development of WoKaS-Iso efforts will focus on expanded spatial coverage and improving data quality through encouraging the sharing of raw data from literatures, reports, internal databases and unpublished records by researchers, institutions and monitoring programs, especially in underrepresented regions such as Africa, South America and Southeast Asia. Enhancements will include more detailed metadata, uncertainty estimates, data quality flags to improve usability. A web-based interface with visualizations is planned to assist data access.

7 Author contributions

YZ and AH collected the karst spring datasets. PCT and YZ contacted data contributors to obtain cave drip water data and aligned this dataset with the SISAL_mon_v1 dataset. YZ designed the structure of WoKaS-Iso database and organized the datasets. YZ digitized data from publication figures. YZ, AH, JGP and FZ contributed to data quality control. KY extracted IsoGSM datasets for each site and YZ performed data extraction from other global products. YZ developed extraction scripts for MSWEP, GLEAM and ERA5, with KOC and XM assisting in code testing. YZ drafted the manuscript under the supervision of AH. All other authors contributed data to the WoKaS-Iso database.

8 Competing interests

The authors declare that they have no conflict of interest.

https://doi.org/10.5194/essd-2025-812
Preprint. Discussion started: 15 January 2026

9 Acknowledgment

Yining Zang acknowledges the financial support from the China Scholarship Council (202207720061). Yining Zang and Andreas Hartmann were supported by the German Research Foundation (DFG, grant number: HA 8113/6–1, project "Robust Conceptualisation of KArst Transport (ROCKAT)"). We want to thank Nikita Kaushal (American Museum of Natural History) for her help in aligning WoKaS-Iso with SISAL_mon_v1, and Qi Li (Robotics Research Lab, University Kaiserslautern-Landau) for assistance in writing global products extraction scripts. We also extend our gratitude to all researchers and institutions who provided data essential for this compilation. In addition, we acknowledge Albert Goede (Retired, formerly University of Tasmania, Australia), Chaojun Chen (No.768, Juxian Street, Chenggong District, Kunming, Yunnan, 650500, China) , Juan Pablo Bernal (Instituto de Geociencias, Campus UNAM Juriquilla, Querétaro, México, 76230), Paul W.Williams (Retired, formerly University of Auckland, School of Environment, Auckland, New Zealand), Quan Wang, Sebastian Breitenbach (Department of Geography and Environmental Sciences, Ellison D116, Northumbria University, Newcastle upon Tyne, NE1 8ST, UK), Yongjin Wang (School of Geography, Nanjing Normal University, Nanjing 210023, China), Yunxia Li (Hunan Normal University, No. 36 Lushan South Road, Changsha 410081, China) for their valuable contribution to both the SISAL_mon_v1 and WoKaS-Iso databases.

References

Allen, S. T., Jasechko, S., Berghuijs, W. R., Welker, J. M., Goldsmith, G. R., and Kirchner, J. W.: Global sinusoidal seasonality in precipitation isotopes, Hydrol Earth Syst Sci, 23, 3423–3436, https://doi.org/10.5194/hess-23-3423-2019, 2019.

Andreo, B., Liñán, C., Carrasco, F., Jiménez de Cisneros, C., Caballero, F., and Mudry, J.: Influence of rainfall quantity on the isotopic composition (18O and 2H) of water in mountainous areas. Application for groundwater research in the Yunquera-Nieves karst aquifers (S Spain), Applied Geochemistry, 19, 561–574, https://doi.org/10.1016/J.APGEOCHEM.2003.08.002, 2004.

Ankit Rohatgi: WebPlotDigitizer, version 4.6, https://apps.automeris.io, 2023.

etopo5: https://pubs.usgs.gov/of/1998/of98-801/bathy/metadata/etopo5.htm, last access: 9 April 2025.

European Cooperation in Science and Technology: Hydrogeological aspects of groundwater protection in Karstic areas: Final report, KIP Articles. 2410, 1995.

Bakalowicz, M.: Karst groundwater: A challenge for new resources, Hydrogeol J, 13, 148–160, https://doi.org/10.1007/S10040-004-0402-9/FIGURES/6, 2005.

Baker, A., Hartmann, A., Duan, W., Hankin, S., Comas-Bru, L., Cuthbert, M. O., Treble, P. C., Banner, J., Genty, D., Baldini, L. M., Bartolomé, M., Moreno, A., Pérez-Mejías, C., and Werner, M.: Global analysis reveals climatic controls on the oxygen isotope composition of cave drip water, Nat Commun, 10, 1–7, https://doi.org/10.1038/S41467-019-11027-W;SUBJMETA, 2019.

https://doi.org/10.5194/essd-2025-812
Preprint. Discussion started: 15 January 2026

Beck, H. E., van Dijk, A. I. J. M., Levizzani, V., Schellekens, J., Miralles, D. G., Martens, B., and de Roo, A.: MSWEP: 3-hourly 0.25° global gridded precipitation (1979–2015) by merging gauge, satellite, and reanalysis data, Hydrol. Earth Syst. Sci., 21, 589–615, https://doi.org/10.5194/hess-21-589-2017, 2017.

Beck, H. E., Pan, M., Roy, T., Weedon, G. P., Pappenberger, F., van Dijk, A. I. J. M., Huffman, G. J., Adler, R. F., and Wood, E. F.: Daily evaluation of 26 precipitation datasets using Stage-IV gauge-radar data for the CONUS, Hydrol. Earth Syst. Sci., 23, 207–224, https://doi.org/10.5194/hess-23-207-2019, 2019a.

Beck, H. E., Wood, E. F., Pan, M., Fisher, C. K., Miralles, D. G., van Dijk, A. I. J. M., McVicar, T. R., and Adler, R. F.: MSWEP V2 Global 3-Hourly 0.1° Precipitation: Methodology and Quantitative Assessment, Bull. Amer. Meteor. Soc., 100, 473–500, https://doi.org/10.1175/BAMS-D-17-0138.1, 2019b.

Birkel, C. and Soulsby, C.: Advancing tracer-aided rainfall–runoff modelling: a review of progress, problems and unrealised potential, Hydrol Process, 29, 5227–5240, https://doi.org/10.1002/HYP.10594, 2015.

Bowen, G. J. and Revenaugh, J.: Interpolating the isotopic composition of modern meteoric precipitation, 39, 1299, https://doi.org/10.1029/2003WR002086, 2003.

Bowen, G. J. and Wilkinson, B.: Spatial distribution of $\delta^{18}O$ in meteoric precipitation, Geology, 315–318, https://doi.org/10.1130/0091-7613(2002)030, 2002.

Bowen, G. J., Wassenaar, L. I., and Hobson, K. A.: Global application of stable hydrogen and oxygen isotopes to wildlife forensics, Oecologia, 143, 337–348, https://doi.org/10.1007/S00442-004-1813-Y, 2005.

Bradley, C., Baker, A., Jex, C. N., and Leng, M. J.: Hydrological uncertainties in the modelling of cave drip-water δ18O and the implications for stalagmite palaeoclimate reconstructions, Quat Sci Rev, 29, 2201–2214, https://doi.org/10.1016/J.QUASCIREV.2010.05.017, 2010.

Chen, Z., Auler, A. S., Bakalowicz, M., Drew, D., Griger, F., Hartmann, J., Jiang, G., Moosdorf, N., Richts, A., Stevanovic, Z., Veni, G., and Goldscheider, N.: The World Karst Aquifer Mapping project: concept, mapping procedure and map of Europe. Hydrogeol J 25, 771–785, https://doi.org/10.1007/s10040-016-1519-3, 2017.

Ford, D. and Williams, P.: Karst Hydrogeology and Geomorphology, Karst Hydrogeology and Geomorphology, 1–562, https://doi.org/10.1002/9781118684986, 2007.

Frank, S., Goeppert, N., and Goldscheider, N.: Improved understanding of dynamic water and mass budgets of high-alpine karst systems obtained from studying a well-defined catchment area, Hydrol Process, 35, e14033, https://doi.org/10.1002/HYP.14033, 2021.

Giese, M., Caballero, Y., Hartmann, A., and Charlier, J. B.: Trends in long-term hydrological data from European karst areas: Insights for groundwater recharge evaluation, Hydrol Earth Syst Sci, 29, 3037–3054, https://doi.org/10.5194/HESS-29-3037-2025, 2025.

Goldscheider, N. and Drew, D.: Methods in karst hydrogeology. International Contribution to Hydrogeology, 264, 2007.

Hartmann, A. and Baker, A.: Modelling karst vadose zone hydrology and its relevance for paleoclimate reconstruction, Earth Sci Rev, 172, 178–192, https://doi.org/10.1016/J.EARSCIREV.2017.08.001, 2017.

https://doi.org/10.5194/essd-2025-812
Preprint. Discussion started: 15 January 2026

Hartmann, A., Kralik, M., Humer, F., Lange, J., and Weiler, M.: Identification of a karst system's intrinsic hydrodynamic parameters: Upscaling from single springs to the whole aquifer, Environ Earth Sci, 65, 2377–2389, https://doi.org/10.1007/s12665-011-1033-9, 2012.

Hartmann, A., Wagener, T., Rimmer, A., Lange, J., Brielmann, H., and Weiler, M.: Testing the realism of model structures to identify karst system processes using water quality and quantity signatures, Water Resour Res, 49, 3345–3358, https://doi.org/10.1002/wrcr.20229, 2013.

Hartmann, A., Goldscheider, N., Wagener, T., Lange, J., and Weiler, M.: Karst water resources in a changing world: Review of hydrological modeling approaches, Rev. Geophys., 52, 218–242, https://doi.org/10.1002/2013RG000443, 2014.

Hartmann, A., Jasechko, S., Gleeson, T., Wada, Y., Andreo, B., Barberá, J. A., Brielmann, H., Bouchaou, L., Charlier, J., Darling, W. G., Filippini, M., Garvelmann, J., Goldscheider, N., Kralik, M., Kunstmann, H., Ladouche, B., Lange, J., Lucianetti, G., Martín, J. F., Mudarra, M., Sánchez, D., Stumpp, C., Zagana, E., and Wagener, T.: Risk of groundwater contamination widely underestimated because of fast flow into aquifers, Proc. Natl. Acad. Sci. U.S.A., 118, e2024492118, https://doi.org/10.1073/pnas.2024492118, 2021.

Hersbach, H., Bell, B., Berrisford, P., Hirahara, S., Horányi, A., Muñoz-Sabater, J., Nicolas, J., Peubey, C., Radu, R., Schepers, D., Simmons, A., Soci, C., Abdalla, S., Abellan, X., Balsamo, G., Bechtold, P., Biavati, G., Bidlot, J., Bonavita, M., De Chiara, G., Dahlgren, P., Dee, D., Diamantakis, M., Dragani, R., Flemming, J., Forbes, R., Fuentes, M., Geer, A., Haimberger, L., Healy, S., Hogan, R. J., Hólm, E., Janisková, M., Keeley, S., Laloyaux, P., Lopez, P., Lupu, C., Radnoti, G., de Rosnay, P., Rozum, I., Vamborg, F., Villaume, S., and Thépaut, J. N.: The ERA5 global reanalysis, Quarterly Journal of the Royal Meteorological Society, 146, 1999–2049, https://doi.org/10.1002/qj.3803, 2020.

Hersbach, Hans., Bell, B., Berrisford, P., Biavati, G., Horányi, A., Muñoz-Sabater, J., Nicolas, J., Peubey, C., Radu, R., Rozum, I., Schepers, D., Simmons, A., Soci, C., Dee, D., and Thépaut, J.-N.: Copernicus Climate Change Service, Climate Data Store, (2023): ERA5 hourly data on single levels from 1940 to present., Copernicus Climate Change Service (C3S) Climate Data Store (CDS), https://doi.org/10.24381/cds.adbb2d47, 2023.

Hulsman, P., Keune, J., Koppa, A., Schellekens, J., and Miralles, D. G.: Incorporating Plant Access to Groundwater in Existing Global, Satellite-Based Evaporation Estimates, Water Resour Res, 59, https://doi.org/10.1029/2022WR033731, 2023.

Jourde, H., Massei, N., Mazzilli, N., Binet, S., Batiot-Guilhe, C., Labat, D., Steinmann, M., Bailly-Comte, V., Seidel, J.L., Arfib, B., Charlier, J.B., Guinot, V., Jardani, A., Fournier, M., Aliouache, M., Babic, M., Bertrand, C., Brunet, P., Boyer, J.F., Bricquet, J.P., Camboulive, T., Carrière, S.D., Celle-Jeanton, H., Chalikakis, K., Chen, N., Cholet, C., Clauzon, V., Soglio, L.D., Danquigny, C., Défargue, C., Denimal, S., Emblanch, C., Hernandez, F., Gillon, M., Gutierrez, A., Sanchez, L.H., Hery, M., Houillon, N., Johannet, A., Jouves, J., Jozja, N., Ladouche, B., Leonardi, V., Lorette, G., Loup, C., Marchand, P., de Montety, V., Muller, R., Ollivier, C., Sivelle, V., Lastennet, R., Lecoq, N., Maréchal, J.C., Perotin, L., Perrin, J., Petre, M.A., Peyraube, N., Pistre, S., Plagnes, V., Probst, A., Probst, J.L., Simler, R., Stefani, V., Valdes-Lao, D., Viseur, S. and Wang, X.: SNO KARST: A French Network of Observatories for the Multidisciplinary Study of Critical Zone Processes in Karst Watersheds and Aquifers. Vadose Zone Journal, 17: 1-18 180094. https://doi.org/10.2136/vzj2018.04.0094, 2018

Kanamitsu, M., and Coauthors: NCEP Dynamical Seasonal Forecast System 2000, Bull. Amer. Meteor. Soc., 83, 1019–1038, https://doi.org/10.1175/1520-0477(2002)083<1019:NDSFS>2.3.CO;2, 2002.

Kaushal, N., Lechleitner, F. A., Wilhelm, M., Azennoud, K., Bühler, J. C., Braun, K., Ait Brahim, Y., Baker, A., Burstyn, Y., Comas-Bru, L., Fohlmeister, J., Goldsmith, Y., Harrison, S. P., Hatvani, I. G., Rehfeld, K., Ritzau, M., Skiba, V., Stoll, H. M., Szűcs, J. G., Tanos, P., Treble, P. C., Azevedo, V., Baker, J. L., Borsato, A., Chawchai, S., Columbu, A., Endres, L., Hu, J., Kern, Z., Kimbrough, A., Koç, K., Markowska, M., Martrat, B., Masood Ahmad, S., Nehme, C., Novello, V. F., Pérez-Mejías, C., Ruan, J., Sekhon, N., Sinha, N., Tadros, C. V., Tiger, B. H., Warken, S., Wolf, A., Zhang, H., and SISAL Working Group members: SISALv3: a global speleothem stable isotope and trace element database, Earth Syst. Sci. Data, 16, 1933–1963, https://doi.org/10.5194/essd-16-1933-2024, 2024.

Koppa, A., Rains, D., Hulsman, P., Poyatos, R., and Miralles, D. G.: A deep learning-based hybrid model of global terrestrial evaporation, Nat Commun, 13, https://doi.org/10.1038/s41467-022-29543-7, 2022.

Labat, D., Sivakumar, B., and Mangin, A.: Evidence for deterministic chaos in long-term high-resolution karstic streamflow time series, Stoch. Environ. Res. Risk Assess., 30, 2189–2196, https://doi.org/10.1007/s00477-015-1175-5, 2016.

Li, G., Chen, X., Zhang, Z., Wang, L., and Soulsby, C.: Effects of passive-storage conceptualization on modeling hydrological function and isotope dynamics in the flow system of a cockpit karst landscape, Hydrol Earth Syst Sci, 26, 5515–5534, https://doi.org/10.5194/hess-26-5515-2022, 2022.

Li, R., Zhu, G., Chen, L., Qi, X., Lu, S., Meng, G., Wang, Y., Li, W., Zheng, Z., Yang, J., and Gun, Y.: Global Stable Isotope Dataset for Surface Water, Earth Syst Sci Data, 17, 2135–2145, https://doi.org/10.5194/ESSD-17-2135-2025, 2025.

Liu, J., Shangguan, D., Liu, S., Ding, Y., Wang, S., and Wang, X.: Evaluation and comparison of CHIRPS and MSWEP daily-precipitation products in the Qinghai-Tibet Plateau during the period of 1981–2015, Atmos Res, 230, 104634, https://doi.org/10.1016/J.ATMOSRES.2019.104634, 2019.

Liu, Y. and Yamanaka, T.: Tracing groundwater recharge sources in a mountain–plain transitional area using stable isotopes and hydrochemistry, J Hydrol (Amst), 464–465, 116–126, https://doi.org/10.1016/J.JHYDROL.2012.06.053, 2012.

Martens, B., Miralles, D. G., Lievens, H., van der Schalie, R., de Jeu, R. A. M., Fernández-Prieto, D., Beck, H. E., Dorigo, W. A., and Verhoest, N. E. C.: GLEAM v3: satellite-based land evaporation and root-zone soil moisture, Geosci. Model Dev., 10, 1903–1925, https://doi.org/10.5194/gmd-10-1903-2017, 2017.

Mayer-Anhalt, L., Birkel, C., Sánchez-Murillo, R., and Schulz, S.: Tracer-aided modelling reveals quick runoff generation and young streamflow ages in a tropical rainforest catchment, Hydrol Process, 36, e14508, https://doi.org/10.1002/HYP.14508, 2022.

McDermott, F.: Palaeo-climate reconstruction from stable isotope variations in speleothems: a review, Quat Sci Rev, 23, 901–918, https://doi.org/10.1016/J.QUASCIREV.2003.06.021, 2004.

McDermott, F., Schwarcz, H., Rowe, P.J.: Isotopes in speleothems. In: Leng, M.J. (eds) Isotopes in Palaeoenvironmental Research. Developments in Paleoenvironmental Research, vol 10. Springer, Dordrecht. https://doi.org/10.1007/1-4020-2504-1_05, 2006.

https://doi.org/10.5194/essd-2025-812
Preprint. Discussion started: 15 January 2026

McDonnell, J. J., McGuire, K., Aggarwal, P., Beven, K. J., Biondi, D., Destouni, G., Dunn, S., James, A., Kirchner, J., Kraft, P., Lyon, S., Maloszewski, P., Newman, B., Pfister, L., Rinaldo, A., Rodhe, A., Sayama, T., Seibert, J., Solomon, K., Soulsby, C., Stewart, M., Tetzlaff, D., Tobin, C., Troch, P., Weiler, M., Western, A., Wörman, A., and Wrede, S.: How old is streamwater? Open questions in catchment transit time conceptualization, modelling and analysis, Hydrol Process, 24, 1745–1754, https://doi.org/10.1002/HYP.7796, 2010.

Miralles, D. G., Holmes, T. R. H., De Jeu, R. A. M., Gash, J. H., Meesters, A. G. C. A., and Dolman, A. J.: Global land-surface evaporation estimated from satellite-based observations, Hydrol Earth Syst Sci, 15, 453–469, https://doi.org/10.5194/hess-15-453-2011, 2011.

Miralles, D. G., Bonte, O., Koppa, A., Baez-Villanueva, O. M., Tronquo, E., Zhong, F., Beck, H. E., Hulsman, P., Dorigo, W., Verhoest, N. E. C., and Haghdoost, S.: GLEAM4: global land evaporation and soil moisture dataset at 0.1° resolution from 1980 to near present, Scientific Data 12, 416, https://doi.org/10.1038/s41597-025-04610-y, 2025.

Nan, Y., He, Z., Tian, F., Wei, Z., and Tian, L.: Can we use precipitation isotope outputs of isotopic general circulation models to improve hydrological modeling in large mountainous catchments on the Tibetan Plateau?, Hydrol Earth Syst Sci, 25, 6151–6172, https://doi.org/10.5194/hess-25-6151-2021, 2021.

Olarinoye, T., Gleeson, T., Marx, V., Seeger, S., Adinehvand, R., Allocca, V., Andreo, B., Apaéstegui, J., Apolit, C., Arfib, B., Auler, A., Barberá, J. A., Batiot-Guilhe, C., Bechtel, T., Binet, S., Bittner, D., Blatnik, M., Bolger, T., Brunet, P., Charlier, J. B., Chen, Z., Chiogna, G., Coxon, G., De Vita, P., Doummar, J., Epting, J., Fournier, M., Goldscheider, N., Gunn, J., Guo, F., Guyot, J. L., Howden, N., Huggenberger, P., Hunt, B., Jeannin, P. Y., Jiang, G., Jones, G., Jourde, H., Karmann, I., Koit, O., Kordilla, J., Labat, D., Ladouche, B., Liso, I. S., Liu, Z., Massei, N., Mazzilli, N., Mudarra, M., Parise, M., Pu, J., Ravbar, N., Sanchez, L. H., Santo, A., Sauter, M., Sivelle, V., Skoglund, R. Ø., Stevanovic, Z., Wood, C., Worthington, S., and Hartmann, A.: Global karst springs hydrograph dataset for research and management of the world's fastest-flowing groundwater, Sci Data, 7, https://doi.org/10.1038/s41597-019-0346-5, 2020.

Pape, J. R., Banner, J. L., Mack, L. E., Musgrove, M. L., and Guilfoyle, A.: Controls on oxygen isotope variability in precipitation and cave drip waters, central Texas, USA, J Hydrol (Amst), 385, 203–215, https://doi.org/10.1016/J.JHYDROL.2010.02.021, 2010.

Priestley, S. C., Treble, P. C., Griffiths, A. D., Baker, A., Abram, N. J., and Meredith, K. T.: Caves demonstrate decrease in rainfall recharge of southwest Australian groundwater is unprecedented for the last 800 years, Commun Earth Environ, 4, 206, https://doi.org/10.1038/S43247-023-00858-7, 2023.

Rusjan, S., Sapač, K., Petrič, M., Lojen, S., and Bezak, N.: Identifying the hydrological behavior of a complex karst system using stable isotopes, J Hydrol (Amst), 577, https://doi.org/10.1016/j.jhydrol.2019.123956, 2019.

Staudinger, M., Seeger, S., Herbstritt, B., Stoelzle, M., Seibert, J., Stahl, K., and Weiler, M.: The CH-IRP data set: A decade of fortnightly data on δ2H and δ18O in streamflow and precipitation in Switzerland, Earth Syst Sci Data, 12, 3057–3066, https://doi.org/10.5194/ESSD-12-3057-2020, 2020.

https://doi.org/10.5194/essd-2025-812
Preprint. Discussion started: 15 January 2026

Stevanović, Z.: Karst waters in potable water supply: a global scale overview, Environ Earth Sci, 78, 662, https://doi.org/10.1007/s12665-019-8670-9, 2019.

Treble, P. C., Baker, A., Abram, N. J., Hellstrom, J. C., Crawford, J., Gagan, M. K., Borsato, A., Griffiths, A. D., Bajo, P., Markowska, M., Priestley, S. C., Hankin, S., and Paterson, D.: Ubiquitous karst hydrological control on speleothem oxygen isotope variability in a global study, Communications Earth & Environment 3, 29, https://doi.org/10.1038/s43247-022-00347-3, 2022.

Tremaine, D. M., Froelich, P. N., and Wang, Y.: Speleothem calcite farmed in situ: Modern calibration of δ18O and δ13C paleoclimate proxies in a continuously-monitored natural cave system, Geochim Cosmochim Acta, 75, 4929–4950, https://doi.org/10.1016/J.GCA.2011.06.005, 2011.

Wang, Z., Su, Q., Wang, S., Gao, Z., and Liu, J.: Coupling hydrochemistry and stable isotopes (δ^2H and δ^{18}O) to identify the major factors affecting the hydrochemical evolution of groundwater in the Western Yellow Sea Coast, China, Applied Geochemistry, 138, 105221, https://doi.org/10.1016/J.APGEOCHEM.2022.105221, 2022.

Yoshimura, K., Kanamitsu, M., Noone, D., and Oki, T.: Historical isotope simulation using Reanalysis atmospheric data, Journal of Geophysical Research Atmospheres, 113, https://doi.org/10.1029/2008JD010074, 2008.

Zang, Y.: The WoKaS-Iso database: workflow for a global compilation of oxygen-18 and deuterium records in karst springs and cave drip water for enhanced understanding of karst systems, OPARA [data set], https://doi.org/10.25532/OPARA-909, 2025.

Zhang, Z., Chen, X., Cheng, Q., and Soulsby, C.: Storage dynamics, hydrological connectivity and flux ages in a karst catchment: Conceptual modelling using stable isotopes, Hydrol Earth Syst Sci, 23, 51–71, https://doi.org/10.5194/HESS-23-51-2019, 2019.

Zhong, F., Jiang, S., Van Dijk, A. I. J. M., Ren, L., Schellekens, J., and Miralles, D. G.: Revisiting large-scale interception patterns constrained by a synthesis of global experimental data, Hydrol Earth Syst Sci, 26, 5647–5667, https://doi.org/10.5194/hess-26-5647-2022, 2022.